New Low GWP Synthetic Refrigerants

Mariam Jarahnejad

Master of Science Thesis EGI-2012-028MSC		
Low GWP Synthetic Refrigerants		
Mariam Jarahnejad		
Approved 2012-05-27	Examiner Professor Björn E Palm	Supervisor Professor Björn E Palm
	Commissioner	Contact person

Abstract

In this project, two newly developed refrigerants, R1234yf and R1234ze have been studied as promising drop-in replacements for the common high global warming potential refrigerants. In view of that, thermodynamic and transport properties of new refrigerants were obtained by RefProp version 7.01 to study and compare their cycle performances with current refrigerants. Furthermore, their environmental and safety aspects have been studied in order to predict probable risks and suitable preparations in different applications. Basic cycle data of both new refrigerants have been calculated for most commonly used condensing and evaporating temperatures. According to evaluation of these tables, both refrigerants generally have comparable COP and volumetric cooling capacity with R134a for an isentropic compression.

As the final phase of the project, drop-in experiment was carried out in a refrigeration cycle consists of two plate heat exchangers and one electrical heater which was placed in the brine loop. Experimentation was operated first by R134a and continued by R1234yf with 10 different brine heat loads at two condensing temperatures of 30°C and 40°C. Subsequently, cycle performance and heat transfer coefficients of R134a and R1234yf were evaluated. Experimental results in heat exchangers were compared with those concluded from theoretical correlations. Outcomes of measurements demonstrate R134a has respectively 2-9.2% and 4.4-15 % higher COP as well as 0-3% and 0-3.8 % higher volumetric cooling capacity than R1234yf at condensing temperatures of 30°C and 40°C.

For calculating heat transfer coefficients of the refrigerants two approaches have been considered. At first approach, modified Wilson plot method has been applied and at the other method, heat transfer coefficient of the secondary refrigerant was evaluated by Talik et al. correlation and subsequently heat transfer coefficients of the refrigerants were computed. Results from the measured data indicate R134a has higher heat transfer coefficients than R1234yf by 4-12% and 9-36% at condenser temperature of 30°C and 40°C respectively.

At the condenser, observations were in agreement with the theoretical correlation and R1234yf had roughly 25% lower overall heat transfer coefficients than R134a.

Table of Contents

Table of Figurers

Nomenclature

A	Effective plate area (m²)
A_x	Flow area (= bw) (m²)
b	Flow channel gap (= p − t) (m)
C_p	Heat capacity at constant pressure (kJ/kgK)
COP	Coefficient of performance of cycle
C_v	heat capacity at constant volume (kJ/kgK)
d_e	equivalent diameter (m)
f	Fanning friction factor
g	Gravitational acceleration (m/s²)
G	Mass flux (kg/m²s)
GWP	Global warming potential
Gz	Graetz number (= Re Pr d_e/L p)
h_{fg}	latent heat (kJ)
h	heat transfer coefficient (W/m²s)
k	thermal conductivity (W/ms)
K	Kelvin
LC50	Lethal Concentration 50% (concentration required to take of life half the people of a tested group)
LD50	Lethal Dose 50 % (dose required to take life of half the people of a tested group)
Lp	effective plate length (m)
NOEL	No Observable adverse effect level
Nu	Nusselt number (= hd_e/k)
ODP	Ozone depletion potential
OEL	Occupational Exposure Limit
p	Perimeter (m)
P_1	Condensing pressure
P_2	Evaporating pressure
P_s	Saturated Pressure
Pcr	Critical pressure
Pr	Prandtl number (= μ c_p/k)
PEL	Permissible exposure limit
Q_L	Heat transfer load (kJ/kg)
q	Heat flux (W/m²)
Re	Reynolds number (= ϱ d_e V/μ)
Rp	Surface toughness (μm)
t	plate thickness (m)
T_1	Evaporating temperature (ºC)
T_2	Condensing temperature (ºC)
TLV	Threshold Limit Value, (maximum permissible exposure level without adverse health effect)
TWA	Time Weighted Average, (average exposure level on basis of eight hours per day)
UA	Overall heat transfer coefficient multiplied by surface (kW/ºC)
V	velocity (m/s)
VCC	Volumetric cooling capacity (kJ/m3)
W	Compressor work (kJ/kg)

Greek Symbols

β	Chevron angle, degrees
λ	Corrugation pitch
ΔP	Pressure drop
μ	Dynamic viscosity
ϱ	Density (kg/m3)
Φ	Enlargement factor (actual area/projected area)

Subscripts

c	Carnot
cond.	Condensing
comp.	Compressor
dis.	Discharge
evap.	Evaporation
l	liquid or laminar
t	Turbulent
w	Wall

1   Introduction

HCFCs (hydrochlorofluorocarbons) and CFCs (chlorofluocarbons) have been applied extensively as refrigerants in air conditioning and refrigeration systems from 1930s as a result of their outstanding safety properties. However, due to harmful impact on ozone layer, by the year 1987 at Montreal Protocol it was decided to establish requirements that initiated the worldwide phase out of CFCs. By the year 1992, the Montreal Protocol was improved to found a schedule in order to phase out the HCFCs. Moreover in 1997 at Kyoto Protocol it was expressed that concentration of greenhouse gases in the atmosphere should be established in a level which is not intensifying global warming ozone layer. Subsequently it was decided to decrease global warming by reduction of greenhouse gases' emissions. (Granryd, et al., 2005)

As a consequence of this protocol even new developed HFCs refrigerants like R-134a should be gradually phased out due to their high global warming potentials. Hence in order to meet the global ecological goals, conventional refrigerants should be replaced by more environmental friendly and safe refrigerants in a way the energy efficiency also is improved.

1.1   Fluid Selection

In refrigeration and air conditioning systems selection of an appropriate working fluid is one of the most significant steps for a particular application. Low global warming potential has been inserted to the long list of desirable criteria of refrigerant's selection. In fact, environmental characteristics of refrigerants are becoming the dominant criteria provided that their thermodynamic behaviors and safeties are favorable as well.

1.1.1   Chemical and thermophysical properties

Generally, thermodynamic and transport properties of refrigerants are the key factors in refrigerant's selection as they determine the performance of the system. The desirable thermodynamic properties are a normal boiling point slightly less than target temperature and, thereby, an evaporating pressure higher than atmospheric pressure. The other favorable characteristics are, low liquid viscosity, high heat of vaporization, modest liquid density and slightly high gas density. It is worthwhile to mention that high heat of vaporization and gas density lead to higher capacity with a specific compressor in a refrigeration system. High liquid thermal conductivity intensifies heat transfer and results in smaller required heat exchangers. Low viscosity also causes low pressure drop in the heat exchangers. Smaller pressure ratio leads lower compression work and improve COP of the system. (Dossat, 1991)

In view of the fact that boiling point and gas density are influenced by the pressure, operating pressure is a factor to choose a suitable refrigerant for a particular application.

Selected refrigerant should be also chemically stable under operation condition while it shouldn't decompose nor react with material in the system.

1.1.2   Environmental impact and safety aspects

Environmental effects are the main problems of common refrigerants so that non environmental friendly impacts of CFCs and later on HCFCs brought about them to be phased out despite of being stable, non-flammable and non-toxic (comparing to Sulfur Dioxide and other refrigerants used before the introduction of CFCs). Ozone depletion potential (ODP) and global warming potential (GWP) are the significant factors demonstrate the direct impact of refrigerants in case of any leakage or releasing to the surroundings. However, using low GWP refrigerants are not the only efficient way to reduce greenhouse gas emissions. In fact it is probable to choose a low GWP refrigerant but still raise total greenhouse gas emissions. When the low GWP refrigerant causes more energy use and fuel consumption actually there are larger indirect emissions. Therefore in developing the low GWP refrigerants always energy efficiency of the system must be studied and its indirect climate impacts should be considered besides its direct emissions. Life cycle climate performance (LCCP) helps to consider overall potential of greenhouse gas

emission of the system including materials, transportation, and operation, production, recycling, servicing and end-of-life. The LCCP (Life Cycle Climate Performance) study is one of the main steps in evaluation of the cradle-to-grave global warming impact of any refrigerant. Furthermore, toxicity and flammability are the determining factors to select suitable refrigerant for any application. Low toxicity and flammability are the most desirable aspects in safety and health studies.

2 Objective

The main aim of the project is to evaluate and assess new refrigerants performances as a drop in replacements for the common high global warming potential refrigerants. Consequently it was necessary to consider thermophysical properties as well as environmental and safety characteristics of the new refrigerants. Hence, basic cycle data of the new refrigerants were provided to have fast estimation of their cycle performances in different temperature conditions. To study heat transfer and cycle performance of the R-1234yf as an alternative refrigerant, drop-in tests were performed in a refrigeration test rig with R134a.

3 Scope

The project is about new developed low global warming potential refrigerants and although available information about developmental refrigerants has been mentioned, mostly thermodynamics characteristics of R1234yf and R1234ze have been studied. R1234yf and R134a have been tested in a refrigeration test rig as well. Experiments were done at two constant condensing temperatures and ten evaporating temperatures. Since quite many experimental data were available about evaporation at the heat exchanger, heat transfer at the evaporator mostly was discussed.

4 Low GWP potential Refrigerant

Lots of studies are being processed and new blends and refrigerants are being developed to substitute conventional refrigerants. Mainly researches have focused on three groups of refrigerants; natural refrigerants, new blends and developing new refrigerants. Natural refrigerants got out of market with coming CFCs and HCFCs but now can be reconsidered. New blends are mixture of mostly natural refrigerants, dimethyl ether (DME) and HFCs in order to combine all advantages of them and achieve the best thermodynamic result and low GWP. Lastly developing a new refrigerant is another solution to overcome the environmental problem. Table 1 compares some characteristics of common and new refrigerants.

Table 1. Comparing properties of different refrigerants.

Refrigerants	Chemical composition	Molecular weight[g/mol]	Critical temperature[°C]	Critical pressure[MPa]	Normal Boiling Point[°C]	Safety class	ODP	GWP
Ammonia (R717)	$N-H_3$	17.02	132.3	11.28	−33.34	B2	0	0
CO2 (R744)	$O=C=O$	44.01	31.03	7.38	-56.6	A1	0	1
Propane (R290)	$CH_3-CH_2-CH_3$	44.096	134.67	4.23	-42.09	A3	0	3
Isobutane (R600a)	$CH_3-CH-CH_3$ CH_3	58.12	134.67	3.65	-11.67	A3	0	3
Propylene (R1270)	$CH2=CH-CH3$	42.08	52.42	4.62	-47.69	A3	0	3
R152a	F_2HC-CH_3	66.05	114	4.76	-24	A2	0	140
R1234ze(E)	Trans, $CHF=CHCF_3$	114.04	79	3.632	-20	A2L	0	6
R1234yf	$CF_3CF=CH_2$	114	95	3.382	-29	A2L	0	4
R134a	CH_2FCF_3	102	101.1	4.059	-26	A1	0	1430

4.1 Natural Refrigerants

4.1.1 Ammonia (R-717)

R-717 is applied widely in large refrigeration systems because of its availability, noticeable heat transfer properties and low cost for large commercial systems. Ammonia can be considered an environmental friendly refrigerant rather than CFCs and HCFCs with zero Global Warming Potential (GWP) and zero Ozone Depletion Potential (ODP). From thermodynamic point of view, R717 is also one of the best options so that its heat transfer coefficient is higher than R22, R11, R12 and R502. (Kilicarslan, 2010)

In addition to its low price, it has relatively high refrigerating capacity per mass as another advantage. Besides its flammability and toxicity, it is not compatible with copper; consequently it cannot be applied in systems with copper pipes. Although it is toxic in high concentration , its sharp smell makes any leakage be detected fast and since it is lighter than air if it leaks it will rise and scatter in the atmosphere. (Korfitsen, 1998)

4.1.2 CO2 (R-744)

CO_2 was one of the most current refrigerants beside ammonia near the beginning of twenty century but it was displaced by CFC and then gradually disappeared from refrigeration systems. Though it is the most familiar greenhouse gas, since its harmful effect is thousands times less than CFCs and HFCs, it was considered again in refrigeration industry. Its non-flammability, zero ozone depletion potential, low toxicity and low global warming potential make it a noticeable alternative for refrigerants with high environmental risks. (Taria et al., 2010)

CO_2 is naturally a substance that can be applied as a working fluid in different heating and cooling applications, due to its excellent heat transfer properties and high volumetric cooling capacity. (Sawalha, 2009)

Its pressure is noticeably higher than R-404a or R-717 which causes to need special design. High pressure leads to high gas density and consequently, higher refrigeration capacity from a given compressor. At low temperatures (-30 to -50 °C) R-744 has a considerable action; for a specified pressure drop, there is a small decrease in saturation temperature, so higher mass flux can be applied in suction pipes and evaporator without any efficiency penalty. (Hrnjak, et al., 2001)

4.1.3 Hydrocarbons

Hydrocarbons were used widely during early years of twenty century as refrigerants but different technical and safety issues lead them to get out of market when CFCs were introduced. Nowadays with the problems resulting from non-environmental friendly refrigerants, they have been considered again as alternative options. Propane (R290), Isobutane (R600a) and Propylene (R1270) are most common sort of HCs used in refrigeration systems. R-1270 and R-290 are applied for heat pumping applications in Europe but R-600a was used in refrigerators and freezers in Europe in the last decade and now it is also applied in Korea and Japan.(Lee, 2005)

Although each of these HCs has different chemical and thermodynamic characteristics, they have common environmental traits; zero ODP and GWP less than 3.

HCs are flammable and classified in range of low toxic, highly flammable refrigerants (A3). They are compatible with almost all of lubricants (except those containing silicone and silicate) which are applied in air conditioning and refrigeration systems. They can be used either in systems designed for specific applications directly or as replacement to other refrigerants along with some modifications. Compatibility with lubricant and safety factors are issues which should be noticed in case of replacements. Currently there are lots of domestic refrigerators and small air conditioning systems which are run by hydrocarbons as refrigerants. HCs also extensively are used in refrigeration process systems in the gas and oil industries. (Arcakliog, 2005)

4.1.4 Hydrocarbon blends

Numbers of low GWP single –component refrigerants which have high critical temperature are limited and most of mixtures that meet these characteristics are zeotropic with large temperature glide. Thus it was decided to evaluate azeotropic blends with thermodynamic properties near to common refrigerants.

ASHRAE published a list of ecofriendly refrigerants which are blends of different natural refrigerants. Mostly they are mixture of hydrocarbons and dimethyl ether (DME, RE170) in which both of them have low GWPs. These new blends are good alternatives for conventional refrigerants with high GWPs .They are drop-in replacements that means with small changes in the system can be replaced with the current high GWP refrigerants. (Davis, 2008)

Table 2 is the list of these new mixtures which has been released by ASHRAE.

Table 2. List of new natural blends as environmental friendly refrigerants (Jung, 2008)

Refrigerants	Composition (% mass)	NBP(°C)	Temperature glide(at 1 atm)	GWP	ODP	Safety class	OEL (ppm)
R-429A	R-E170/R-152a/R-600a(60/10/30)	-25.9	0.5	14	0	A3	1000
R-430A	R-152a/R-600a(76/24)	-27.6	0.2	107	0	A3	1000
R-431A	R-290/R-152a(71/29)	-43.2	0.0	43	0	A3	1000
R-432A	R-1270/R-E170(80/20)	-46.4	1.2	< 3	0	A3	710
R-433A	R-1270/R-290(30/70)	-44.5	0.4	< 3	0	A3	880
R-435A	R-E170/R-152a(80/20)	-26.0	0.2	30	0	A3	1000
R-436A	R-290/R-600a(56/44)	-34.3	8.2	< 3	0	A3	1000
R-436B	R-290/R-600a(52/48)	-33.3	8.3	< 3	0	A3	1000
R-433B	R-1270/R-290(5/95)	-42.6	0.1	< 3	0	N/A	N/A
R-433C	R-1270/R-290(25/75)	-44.2	0.4	< 3	0	N/A	N/A
R-510A	R-E170/R-600a(88/12)	-25.1	0.0	< 3	0	A3	1000

4.2 R-152a (HFC Refrigerant)

R-152a is the only HFC refrigerant that still can be considered as an alternative for R-134a in air conditioning systems. While its GWP is about 130, its chemical properties are like those for R-134a, thus it could be used in existing production system with just some small changes.

R152a has 10% of GWP for R-134a with smaller refrigerant charge than R134a, in the other words at systems with R-152a as working fluid; refrigerant charge is about 35% lower than that for R-134a. Due to its larger molecules in comparison with R-134a, R152a has less refrigerant leakage. It has been proposed as a "drop-in "replacement for R-134a. (Mathur, 2003)

R-152a is mildly flammable. One way to decrease the flammability risk is to reduce the refrigerant charge in the system. Hence R152a can be detained in a compact refrigeration system in order to decrease its risk to ignite. Also using a compact heat exchanger with mini/micro channels reduces internal system volume and therefore the charge inside the refrigeration system can be reduced. (Hamdar, 2010)

4.3 New refrigerants

4.3.1 HFO-1234ze

HFO-1234ze can be considered a near drop-in replacement of R 134a. Its thermodynamic behavior is similar to the R-134a. It is non-flammable which make it safe in refrigeration application. It has very low GWP. It table 3 some of its fundamental properties have been written. (Akasaka, 2009)

It has zero ozone depletion and GWP of 6 which is really lower than refrigerants commonly applied for many heat pumps and refrigerators.

Table 3. Thermodynamic properties For HFO-1234ze (E). (Akasaka, 2009)

Chemical formula	Trans, CHF=CHCF$_3$
Molecular weight (kg/kmol)	114.04
GWP	6
ODP	0
Vapor Pressure at 25°C[Mpa]	0.49
Atmospheric Life Time [day]	18
Vapor Pressure at 50°C[MPa]	1.080
Critical Temperature[°C]	79
Critical Pressure[MPa]	3.632
Critical density[kg/m^3]	486
Normal Boiling Point[°C]	-20
Flame limit	None to 30°C
Lower Flammability Limit[vol.% in air]	-
Upper Flammability limit[vol.% in air]	-
Ignition Temperature[°C]	288 - 293
Minimum Ignition Energy[mJ]	No Ignition at 20°C, 61,000-64,000 at 54°C
Liquid Density at 25°C[kg/m^3]	1180
Acentric Factor	0.296

4.3.2 Thermodynamic properties:

The experimental thermodynamic properties are useful for developing exact equations of state to predict thermodynamic traits of new refrigerants. Figure 1 shows the vapor pressure diagram of some different refrigerants including the HFO-1234ze.
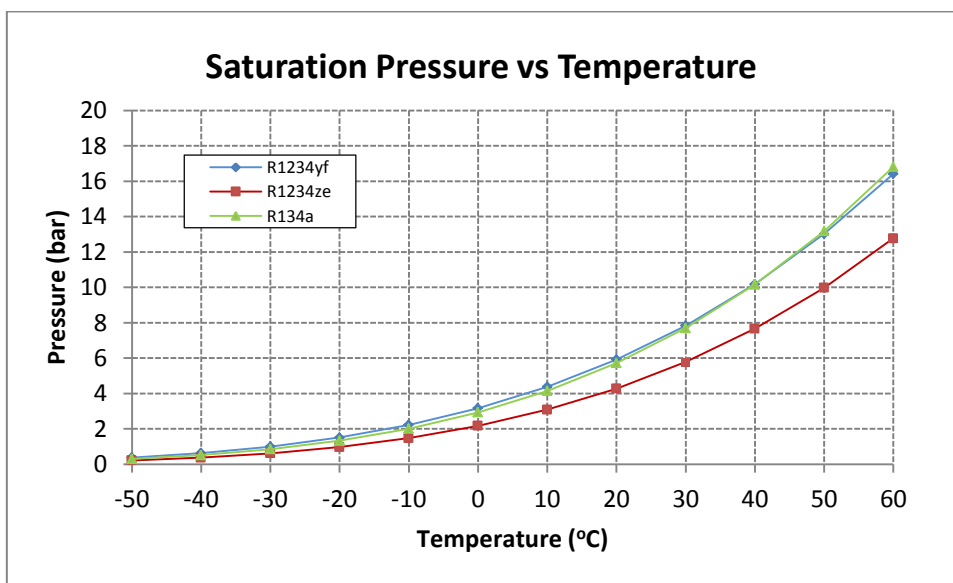
Figure1. Vapor pressure diagram for HFO-1234ze in comparison with some other refrigerants.

For calculation of the cycle performance of refrigeration systems enthalpy-pressure diagrams are necessary. To produce them, dependable equations of state are required. Hence various thermodynamic properties measurements are necessary to develop accurate equations of state. In view of that, in National Defense Academy of Japan, measurements were carried out to evaluate C_v of HFO-1234ze at pressure up to 30MPa and in a temperature range from 3 °C to 152 °C. The gas chromatographic analysis confirmed high purity of 0.9996 mole fraction for the used sample. The calorimeter applied for these measurements is an adiabatic type and consists of a twin-cell structure. The results can be seen at table 4. (Matsuguchi, 2010)

Table 4. Experimental thermodynamic properties for HFO-1234ze (E). (Matsuguchi, 2010)

T (°C)	P(MPa)	ϱ (g/cm3)	C_v(J/gK)	T (°C)	P(MPa)	ϱ (g/cm3).	C_v(J/gK)
-3	5.540	1.2666	0.941	82	7.582	1.0471	1.052
2	7.679	1.2662	0 940	87	8.633	1.0469	1.042
7	9.813	1.2657	0.947	92	9.684	1.0466	1.039
12	11.937	1.2653	0.946	97	10.734	1. 0463	1.0438
17	14.055	1.2649	0.942	102	11.784	1.0461	1.044
22	16.163	1.2644	0.940	107	12.833	1.045S	1.060
22	2.684	1.1850	0.968	112	13.882	1.0456	1.061
27	4.524	1.1847	0.975	117	14.930	1.0453	1.056
32	5.963	1.1843	0.977	122	15.976	1. 0450	1.071
37	7. 598	1.1840	0.984	112	4.344	0.7175	1.717
42	9.231	1.1836	0.982	117	4.695	0.7174	1.691
47	10.852	1.1833	0.990	122	5.051	0.7173	1.667
52	12.483	1.1829	0.986	127	5.410	0.7171	1.626
57	14.103	1.1825	0.992	132	5.772	0.7170	1.589
62	15120	1.1822	0.982	137	6.137	0.7169	1.546
62	3.368	1.0482	1.077	142	6.503	0.7168	1.529
67	4.423	1.0479	1.066	150	6.872	0.7167	1.501
72	5.477	1.0477	1.069	152	7.243	0.7166	1.469
77	6.529	1.0474	1.061				

Thermal conductivity of HFO-1234ze and its mixture with R-32 has been calculated as well. The result of the experiment shows that its thermal conductivity is almost 30% lower than R-32 and the mixture of 50/50 mass % has thermal conductivity between R-32 and HFO-1234ze. (Miyara, 2010)

In view of studying thermophysical properties of R1234ze, Dr. Brown and his colleagues have done a study and predicted thermodynamic properties of eight olefins. Peng Robinson equation of state was applied to calculate the temperature-entropy and pressure-enthalpy state charts for HFO-1234ze in figure 2. (Brown, 2009)
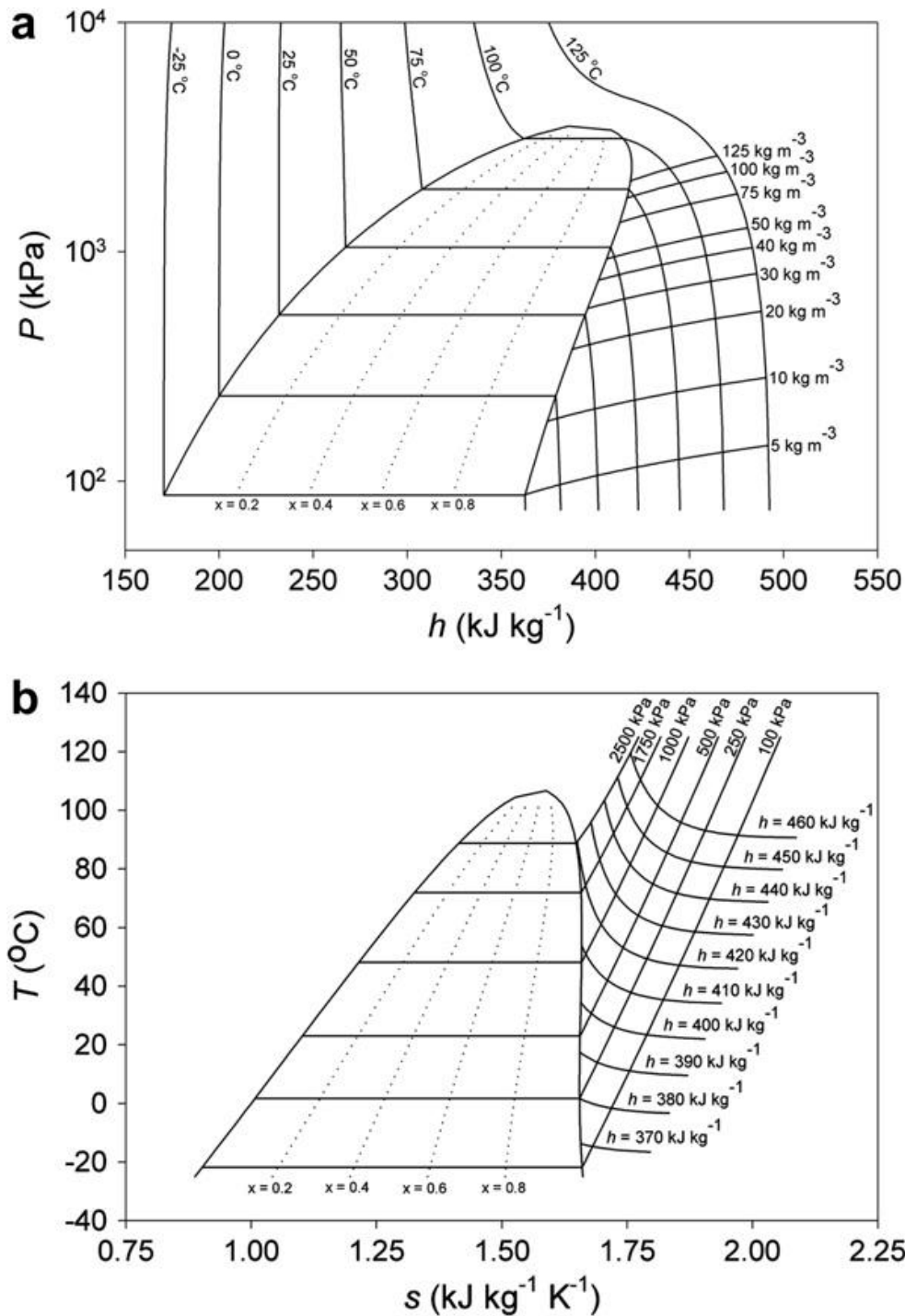
Figure 2. a. Pressure vs. Enthalpy diagram for HFO-1234ze.

b. Temperature vs. Entropy for HFO-1234ze. (Brown, 2009)

4.3.3 Cycle performance

R1234ze (E) is developed as foam blowing agent (Schustera, 2009) and has the potential to be applied in adsorption as the refrigerant. (Skander et al., 2011)

Experiments show HFO-1234ze (E) is a good choice as a replacement refrigerant in turbo refrigeration system. According to experimentations done in a turbo refrigeration system, as it is observed in table 5, although the COP of HFO-1234ze is about 0.2% higher than R-134a, its refrigeration effect is 25% less

than R-134a. This signifies that HFO-1234ze (E) can be a good candidate for turbo refrigeration system if a larger turbo-compressor is applied in comparing with that of R-134a. (Koyama, 2010)

Table 5. COP of HFO-1234ze (E) in comparison with R-134a in a turbo refrigeration system (Koyama, 2010)

Refrigerants	R-134a	HFO-1234ze(E)
Condensation Temperature [ºC]	38	38
Evaporation Temperature [ºC]	6	6
Degree of subcooling [K]	5	5
Degree of superheating [K]	0	0
Efficiency of Compressor	0.85	0.85
Refrigeration effect [kJ/kg]	173.12	157.65
Volumetric refrigeration effect [kJ/m3]	3067.2	2304.8
COP	6.85	6.87
COP ratio (vs. R-134a)	1.00	1.00
Vol. refrigeration capacity [USRt/(m3/s)]	872.1	655.3
Vol. refrigeration capacity ratio (vs. HFC-134a)	1.00	0.75
GWP	1300	6

It was verified that combination of HFO-1234ze with R-32 can be a suitable replacement for R-410A at heating condition. The COP of the HFO-1234ze (E) is 6% higher than R410A but its volumetric cooling capacity is 32% lower. For improving the volumetric refrigeration capacity it is possible to add R-32 to HFO-1234ze (E) while its COP still remains high. However, the notable point is this zeotrop combination could deteriorate heat exchange performance in condenser and evaporator. In table 6, COP for domestic air conditioning system with different proportion of HFO-1234ze (E) and R-32 were calculated and compared to R-410A .(Koyama, 2010)

Table 6. Cycle Performance for an air conditioning system (Koyama, 2010)

Refrigerants	R-410A	HFO-1234ze(E) /R-32		
		100%mass HFO	80%mass HFO	50%mass HFO
Condensation Temperature [ºC]	27	27	27	27
Evaporation Temperature [ºC]	-3	-3	-3	-3
Degree of subcooling [K]	0	0	0	0
Degree of superheating [K]	3	3	3	3
Efficiency of Compressor	0.85	0.85	0.85	0.85
Evaporating pressure [MPa]	0.725	0.193	0.341	0.521
Condensing pressure [MPa]	1.886	0.583	0.994	1.428
Refrigeration effect [kJ/kg]	174.12	144.65	172.35	201.81
Volumetric refrigeration effect [kJ/m³]	4736.0	1509.3	2577.7	3698.4
Compression work [kJ/kg]	31.98	24.65	29.65	35.46
COP $_{heating}$	6.45	6.87	6.81	6.69
COP $_{heating}$ ratio(vs. R410A)	1.00	1.07	1.06	1.04
Volumetric refrigeration capacity [USRt/(m3/s)]	1346.6	429.1	732.9	1051.6
Vol. refrigeration capacity ratio (vs. R410A)	1.00	0.32	0.54	0.78
GWP	1730	6	135	328

The cycle performance of HFO-1234ze(E) is just about 7% better than that of R410A while its volumetric refrigeration capacity is considerably lower than R410A. By adding R-32 into HFO-1234ze(E), the volumetric refrigeration capacity is increasing where the cycle performance is still remained high. It looks as the combinations of HFO-1234ze and R-32 is a good alternative for R410A in domestic heat pump systems and HFO-1234ze also is a suitable candidate for turbo refrigeration system. (Koyama, 2010)

Data in table 7 were calculated in a medium temperature refrigerator in Honeywell Company to investigate the possibility of replacing these new refrigerants in a cycle working with R-134a. At the same thermodynamic condition in both heat exchangers, HFO-1234ze has the same COP as R134a and in spite of lower volumetric cooling capacity, which is a disadvantage, a cycle working with HFO1234ze benefits from lower discharge pressure and temperature. Eventually it can be concluded that HFO-1234ze(E) is a near drop in replacement for R-134a, nevertheless more studies regarding total energy efficiency of the system are necessary. (Fleischer, 2010)

Table.7 Thermodynamic cycle, comparison of R1234yf and R-1234ze to R-134a (Fleischer, 2010)

	Parameter	R134a	R1234ze	R1234yf
Cycle Initial Information	Evap Temperature. [°C]	-6.50	-6.50	-6.50
	Degree of superheating [K]	5.55	5.55	5.55
	Cond. Temperature [°C]	45.00	45.00	45.00
	Degree of subcooling [K]	5.55	5.55	5.55
	Compressor efficiency	0.60	0.60	0.60
Thermodynamic Analysis	P evap. [kPa]	229.8	164.3	249.5
	P cond. [kPa]	1159.9	864.2	1134.1
	Discharge Temperature [°C]	77.5	72.3	64.3
	COPc	2.5	2.5	2.4
	Density of gas phase [kg/m³]	11.1	8.8	13.7
	Compression Ratio	5.0	5.3	4.5
Relative Properties to R-134A	Capacity	100%	73%	94%
	COP	100%	100%	96%
	Suction Pressure	100%.	71%	109%
	Discharge Pressure	100%.	75%	98%.
	Discharge Temperature	0.00	-5.20	-13.27
Other	GWP	1410	6	4
	Flammability	1	None to 30°C	2L
	Toxicity	A	A	A

4.3.4   Safety aspects:

By EU Test method A-11 and ASTM E-681, it was proved that HFO-1234ze is a non-flammable gas. (Honeywell, 2008). Since the risky corrosive and toxic decomposition takes place in case of fire, it is seriously recommended to avoid overheating, sparks and flames. Pyrolysis of HFO-1234ze produces materials containing hydrogen fluoride and fluorocarbons which are the hazardous products. Furthermore it should be kept away from reaction with alkali metals.

According to table 8, in case of leakage there wouldn't observe any harmful effects on biodiversity and also it can be concluded that R1234ze is not categorized as a toxic material. Finally it is notable to mention that this substance is not easily biodegradable. (MSDS, 2008)

Table 8. Important Toxicity Information. (MSDS, 2008)

Test		HFO-1234ze
Cardiac sensitization		NOEL>120,000 ppm
13 Week inhalation		Test completed
Genetic Toxicity	Mouse micronucleus	Not active at 100,000 ppm
	Ames assay	Not active at 50,000 ppm
Toxicity to fish		No Observed Effect Concentration
Toxicity to aquatic plants		No Observed Effect Concentration

4.3.5   HFO-1234yf

HFO-1234yf has been developed as a replacement for HFC-134a in automobile air conditioning as well. Because of its low GWP, favorable LCCP and zero Ozone Depletion Potential (ODP), this new refrigerant has got considered largely by automobile manufactures .It has a good compatibility with existing technology that leads to fast global adoption. Its system performance is similar to R-134a and has comparable COP and cooling capacity to those of R134a. Being thermally stable is another notable property of this new refrigerant which makes it a promising candidate to substitute R-134a. (Tanaka, 2010)

Table 9 is a summary of the properties of HFO-1234yf and HFCF-134a and it can be seen this new developed refrigerant has close thermodynamic properties to R134a despite of its higher flammability.

Table9. Properties of HFO-1234yf and HFCF-134a. (Koban, 2009)

	HFO-1234yf	HFC_134a
Chemical formula	CF3CF=CH2	CH2FCF3
Safety Class	A2L	A1
GWP	4	1430
ODP	0	0
Molar mass [kg/kmol]	114.04	102.3
Critical pressure [MPa]	3.382	4.0593
Critical Temperature [°C]	95	102
Normal Boiling Point [°C]	-29	-26
Atmospheric Life Time [year]	<0.05 (11 day)	14
Lower Flammability Limit [vol.% in air-23ºC]	6.2	-
Upper Flammability limit [vol.% in air-23ºC]	12.3	-
Auto ignition Temperature [°C]	405	>750
Minimum Ignition Energy [mJ]	5000-10000	-
Heat of Combustion [kJ/g]	10.7	4.2
Acute Toxicity Exposure Level [ppm]	101,000	50,000
Molecular Weight [kg/kmol]	114	102
Vapor Density at 25°C [kg/m3]	4.7508	4.2439
Vapor Cp at 25°C [kJ/kgK]	0.92811	0.85118

4.3.5.1 Thermodynamic properties

Tanaka and his collage, Higashi have measured the thermodynamic properties of HFO-1234yf. Patel Teja equation of state and the extended corresponding state (ECS) model have been used to calculate thermodynamic property modeling for this new refrigerant as well. The data are generated by extended corresponding state (ECS) model. The uncertainties with this model are 0.5% in compressed liquid densities, 2.5% in isobaric heat capacities and 0.2% in vapor pressures. Heat capacity and density can be calculated with suitable accuracy with ECS model. (Tanaka, 2010)

Table 10.Saturation densities of HFO-1234yf near the critical point. (Tanaka, 2010)

T (°C)	ϱ (kg/m³)	T (°C)	ϱ (kg/m³)
83.007	195.5	94.85	437.62
86.494	221.3	94.848	478.32
88.584	247.3	94.847	484.3
91.294	279.9	94.81	529.4
91.83	299.1	94.596	553.6
92.758	312.8	94.294	577.9
93.398	326.5	93.607	612.7
93.843	345.9	91.802	669.9
94.008	354.1	87.603	731.4
94.257	378.4	83.595	775.6
94.739	413.1[a]	75.047	848.2
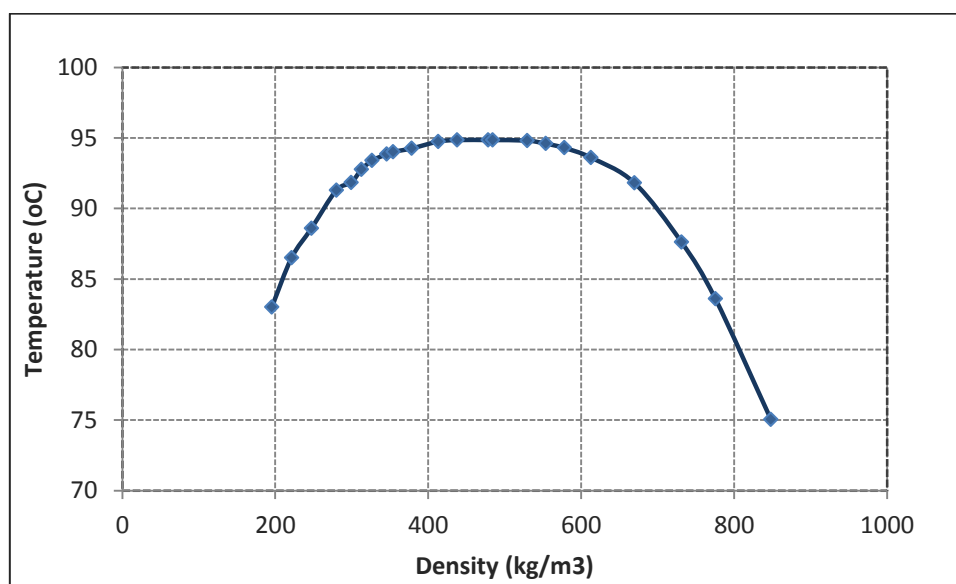
Figure 3. Saturation density of HFO-1234yf near the critical point. (Tanaka, 2010)

For measuring the vapor pressure a batch type calorimeter with a metal bellows was used. The pressure of the HFO-1234yf inside the metal-bellows was balanced with the pressure of nitrogen outside the metal –

bellows. The uncertainty of the experiments is around 1 kPa. Table 11 depicts the measured vapor pressure of R1234yf. For measuring the surface tension, differential capillary rise method has been used. The uncertainty of the measurement is approximately 0.2 (mN/m). The result of the measurement is shown in table 12.

Table 11.Vapor pressure for HFO-1234yf (Tanaka, 2010)

T(^{o}C)	P_s (kPa)	T (^{o}C)	P_s (kPa)
37	939.7	67	1913.9
42	1069.0	72	2128.8
47	1210.3	77	2363.3
52	1362.6	82	2617.0
57	1530.8	87	2893.8
62	1714.0		

Table 12. Surface tension for HFO-1234yf. (Tanaka, 2010)

T(^{o}C)	Surface tension(mN/m)	T(^{o}C)	Surface tension(mN/m)	T(^{o}C)	Surface tension(mN/m)
0	9.30	5.23	8.76	64.77	1.85
5.13	8.68	15.46	7.45	0.25	9.26
16.11	7.33	15.45	7.42	10.16	8.10
27.61	5.78	27.89	5.76	20.59	6.74
35.00	5.08	27.914	5.85	29.70	5.69
45.20	3.82	27.73	5.87	39.30	4.59
54.77	2.80	34.92	4.98	49.48	3.44
65.38	1.82	34.92	4.98	61.19	2.31
0.21	9.23	44.31	3.96	61.20	2.33
5.21	8.67	54.83	2.84		

HFO-1234yf pressure-enthalpy diagram is plotted in figure 4 by RefProp program version 7.01 (Lemmon et al., 2010). Enthalpy and entropy for reference state for saturated liquid was 200 (kJ/kg) and 1 (kJ/kg.K) at 0°C respectively. FEQ Helmholtz equation of state has been applied in RefProp program for thermodynamic properties of R1234yf. (Richter et al., 2010)
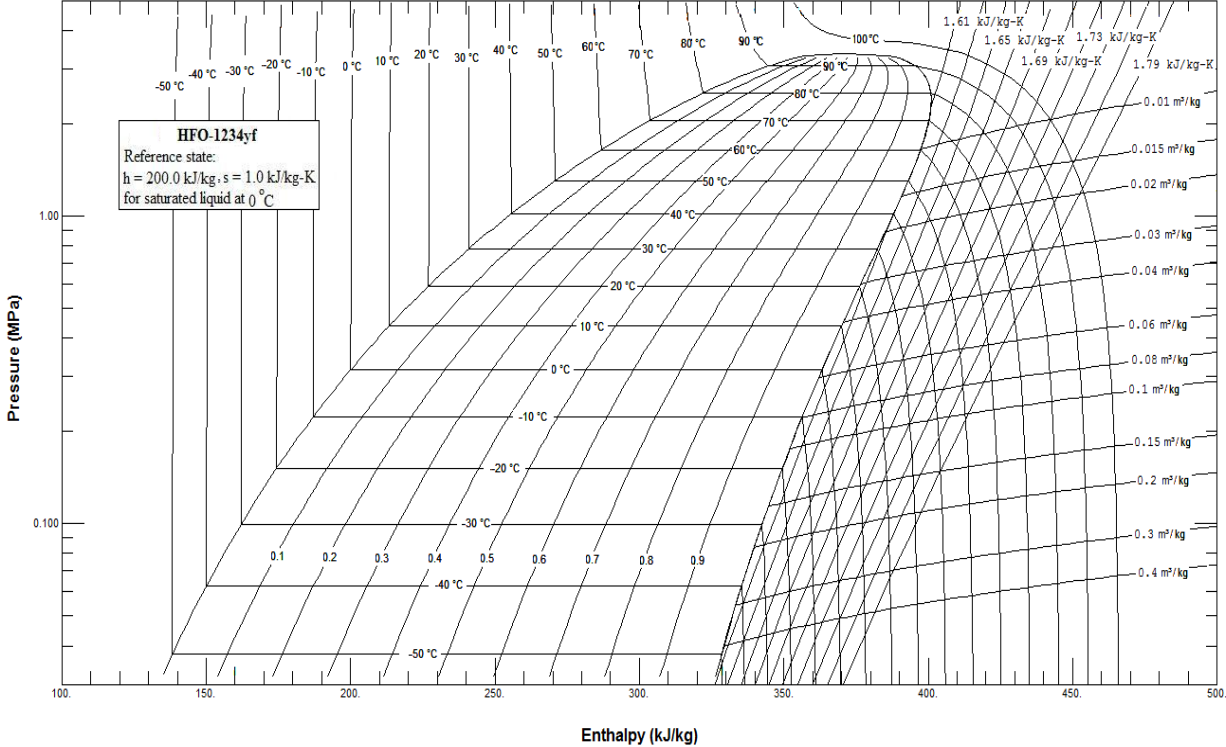
Figure 4. Pressure-Enthalpy graph for HFO-1234yf. (Jarall, 2010)

4.3.6 Cycle Performance

In an experiment done by Dr. Thomas Leck in DuPont Company as a cycle model for ice cream vending machine, capacity and COP for both HFO-1234yf and R-134a have been measured .Table 13.shows that cycle performance and capacity of HFO-1234yf is favorably near to R-134a. The compressor suction temperature is 15°C for both temperatures' conditions. At higher condenser temperature the COP of the system when used R1234yf have decreased slightly while cooling capacity ratio still stayed considerably high. (Leck, 2009)

Table 13. Comparison of volumetric capacity and COP of a vending machine used R-134a and HFO-1234yf as working fluid. (Leck, 2009)

Refrigerant	Evaporator T(°C)	Condenser T(°C)	Capacity (kJ/m³)	Capacity ratio	COP	COP ratio
HFO-1234yf	-12	35	1353.4	99.32%	3.064	97.95
R-134a	-12	35	1362.6		3.128	
HFO-1234yf	-12	47	1167.15	99.43%	2.191	95.68
R-134a	-12	47	1210.3		2.29	

In another study done in Dupont Fluorochemicals R&D by Kontomaris et al., performance of a typical chiller cycle was studied. Calculating the theoretical refrigeration capacity of HFO-1234yf at condensation and evaporation temperatures of 37.8ºC and 4.4ºC respectively shows 7% reduction to R134a. The COP of HFO-1234yf is 4% less than that for R-134a (table 14). It was suggested to apply a larger compressor for using R1234yf in order to achieve the same capacity as with R-134a, even if it is possible to use existing equipment for replacing HFO-1234yf. (Kontomaris et al., 2010)

Table 14. A typical centrifugal chiller performance for HFO-1234yf in comparison with R-134a. (Kontomaris, 2010)

Refrigerant	Compression ratio	Volumetric refrigeration capacity % Δ vs.R-134a	COP % Δ vs R-134a
R-134a	2.795	0	0
HFO-1234yf	2.6	-7	-4

HFO-1234yf has the same operating conditions as R-134a and also similar pressure-temperature curve to R-134a. Its cooling capacity is rather equivalent to R-134a.

4.3.6.1 Safety aspects

HFO-1234yf (2,3,3,3-Tetrafluoropropene) in high temperature can be decomposed and forms hydrofluoric acid (HF) and probably carbonyl fluoride(COF2). If COF_2 contacts with water, it would convert to CO and CO_2.The probability of forming hydrofluoric acid is the same for R-134a. The amount of generated HF is extremely dependent on the area and duration of contact with hot surface or open flame. But in fact during years of using R-134a in automobile air conditioning not so many published medical reports regarding to HF exposures have been seen, thus it can indicate HFO-1234yf is safe in mobile air conditioning applications as well. (Fact Sheet, 2011)

HFO-1234yf is neutral and a stable gas and no harmful polymerization happened at normal condition. It is not biodegradable so it should be avoided from discharge in the environment. There would be undesired reactions in case of contact with strong acids and bases and also oxidizing agents. Table 15 illustrates these materials examples which are not compatible with R-1234yf and it should be avoided to use in construction of the system working with R-1234yf

Table 15. Incompatible Material with HFO-1234yf. (MSDS, 2010)

Incompatible Materials	Examples
Strong Lewis acids	Aluminum chloride
Strong reducing agents	Alkali metals (lithium, potassium sodium), Powdered aluminum, zinc or magnesium. Alkaline-earth metals(calcium magnesium)
Strong bases	Potassium hydroxide
Oxidizing agents	ozone hydrogen peroxide, bleach, bromine, chlorine.

According to ASTM E681 it is slightly flammable but considerably less than R-32 and R-152a. As figure 5 shows HFO-1234yf has high Minimum Ignition Energy which means it is difficult to ignite and also burning velocity about 1.5cm/s indicates slow flame. The flammability characteristics of different refrigerants are also compared it figure 5. As can be seen, despite of greater flammability than R134a, HFO-1234yf has milder flammability characteristics than hydrocarbons and the other current refrigerants.

Furthermore, higher required ignition energy and lower burning velocity result in lower flammability risk relative to the other mentioned refrigerants .(Koban, 2010)
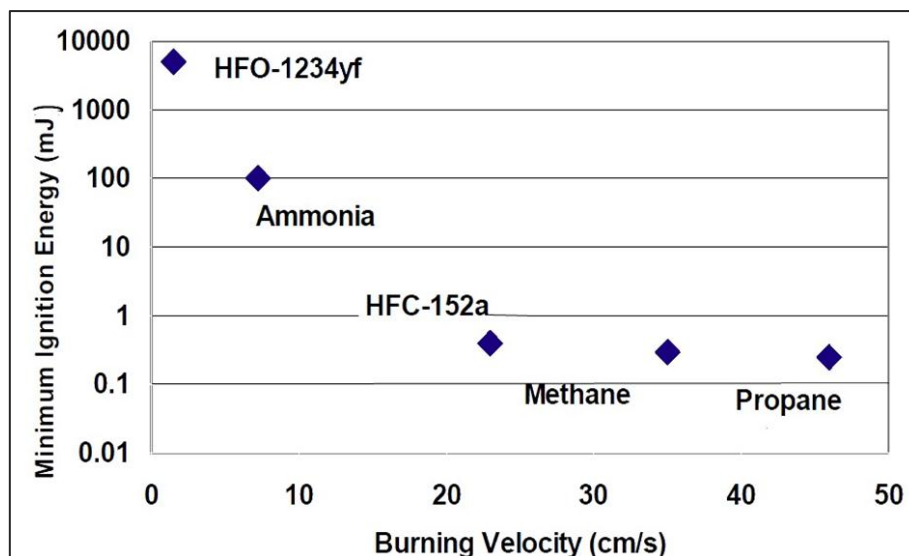
Figure 5. Flammability behavior of R-1234yf in comparison with the other known refrigerants. (Koban, 2010)

HFO-1234yf has low acute toxicity like to R-134a. Long term toxicity test results are favorable and the equipment and requirements at health centers and manufactories could be the same as current refrigerants. Table 16 shows the noticeable toxicity data about HFO-1234yf and compares it with R-134a.The outcome of analyzing this information indicates that HFO-1234yf has low chronic and acute toxicity similar to R-134a. According to various toxicology tests' results, it has been concluded that HFO-1234yf is safe to use in mobile air conditioning applications. (Toxicity Summary, 2010)

Table 16. Important Toxicity information. (Toxicity Summary, 2010)

Test	HFO-1234yf	R-134a
Acute Lethality	No decease 400,000 ppm	No decease 359,700 ppm
Cardiac sensitization	NOEL>120,000 ppm	NOEL 50,000 PPM
13 Week inhalation	NOEL 50,000 ppm	NOEL 50,000 ppm
Genetic Toxicity	Not Mutagenic	Not Mutagenic
13 week genomic (carcinogenicity)	Not active (50,000 ppm)	Baseline (50,000 ppm)
Environmental Toxicity	NOEL >100 mg/L (acceptable)	NOEL >100 mg/L (acceptable)

4.3.6.2   Environmental Aspect

Environmental impacts usually come about when refrigerant leaks from the equipment. The atmospheric effects of this new refrigerant have been considered about its impacts on climate change, local air quality, stratospheric ozone and ecosystems which in the latter case, formation of toxic or lethal degradation products have been studied (SAE, 2009).

Degradation of HFO-1234yf in atmosphere is started by reaction with hydroxy (OH) radicals. Main products of this oxidation reaction which have significant role in air pollution are trifluoric acid (TFA), hydrofluoric acid (HF) and CO2. (Benni, 2009).TFA is a natural element of the hydrosphere and find in

the ocean in huge quantities .It is biodegradable and stable under normal condition and doesn't accumulate in organisms' bodies. The amount of TFA which is produced from degradation of HFO-1234yf is considerably below predicted No Observed Effect Concentration (NOEC) thresholds and will not affect ecosystems. (Atkinson, 2008)

Another product is CO_2 which enhances greenhouse impact but has formed in small quantities and degrades by photosynthesis. HF would rain out of the atmosphere and reacts with calcium sulfate and produces sulphuric acid and calcium fluoride. (Kajihara, 2010)

Its GWP and atmospheric life time are well acceptable and there is no main contribution to radiative forcing of climate changing. HFO-1234yf doesn't have bromine or chlorine (Nielsen, 2007), so it doesn't contribute to catalytic ozone destruction cycle and no significant stratospheric impacts have been seen. Finally results show no significant atmospheric concerns and impacts. (Hill, 2010)

Several LCCP evaluations show HFO-1234yf provided remarkable decreases (17-20%) to overall CO_2-equivalent emissions compared to HFC-134a.It seemed this new developed refrigerants is a noticeable alternative at least for R-134a. (Koban, 2009)

4.3.7 HDRs

In some applications higher volumetric capacity are desired. These include most air conditioning and some larger refrigeration systems. Evaluation of blends which provide both greater capacity and low GWP are favorable. However, it is significant that these working fluids have high energy efficiency and reasonable cost. In Honeywell Company new lower GWP blends named HDR, are processing so that there would be no major change in safety and energy efficiency of the existing systems. HDR-01 and HDR-07 are mixtures while having close operating characteristics to R-407C, their GWP are less than 150. Other Honeywell developmental refrigerants are HDR-06 and HDR-11 which have similar vapor pressure to R-410A. Their GWP are slightly less than 500 but they also have lower volumetric capacity than given refrigerants like R-410C.

In a presentation from Honeywell, it is mentioned that all the studied blends are mildly flammable. Even if they have noteworthy properties, more data and experimental evaluations are necessary to discuss them comprehensively. (Samuel, 2010)

4.3.8 DR-11

DR-11 has recently been developed by Dupont. It is a new blend based on HFO-1234yf with close thermodynamic properties and cycle performance to R-134a. It is commercially named Opteon XP10. It is non-flammable with GWP near to 600 and temperature glide less than 0.01°C. It is worthwhile to mention that its composition is undisclosed. Experiments show it is an appropriate and cost effective candidate for commercial refrigeration system using R134a. Table 17 compares some properties of DR-11 to R-134a.

Table 17. Thermodynamic properties of DR-11, HFO-1234yf and R-134a.

	DR-11	HFO-1234yf	HFC-134a
Chemical formula	Undisclosed	$CF_3CF=CH_2$	CH_2FCF_3
Safety Class	A1	A2L	A1
GWP	less than 600	4	1430
ODP	0	0	0
Critical Temperature[°C]	97.5	95	102
Critical pressure [MPa]	3.82	3.382	4.056
Normal Boiling Point [°C]	-29.2	-29	-26

Lower Flammability Limit [vol.% in air]	-	6.5	-
Upper Flammability limit [vol.% in air]	-	12.3	-
Auto ignition Temperature [°C]	-	405	>750

More studies and experiments revealed this new refrigerant can be used as medium temperature working fluid beside CO_2 at the low temperature side in hybrid systems. It is also concluded that in such a system there would be 90% reduction in direct carbon emission and 50% in entire carbon emission compared to the current food retailer's refrigeration system using R404A in a direct expansion system. Different laboratory tests are still under way to determine its performance in water chillers, medium temperature refrigeration and commercial air conditioning.

Dupont Company has decided to market it in the EU during 2012 and 2013 in a limited quantity and then access the market interest to decide the best time to commercialize it. (Reimer, 2010)
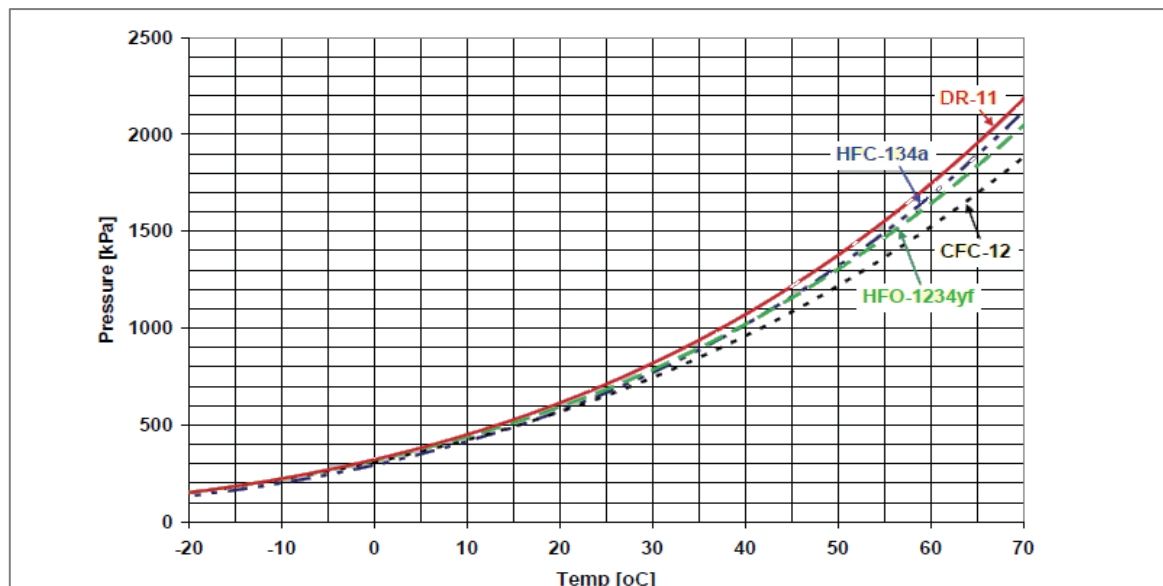
Figure 6.Vapor pressure diagram for DR-11, HFO-1234yf and R134a. (Hughes et al., 2010)

In figure 6 vapor pressure curve of DR-11 is compared with some other refrigerants. According to predicted thermodynamic cycle performance of DR-11 by Dupont Company showed in table 18, it seems this refrigerant has a greater volumetric cooling capacity and COP than HFO-1234yf and its thermodynamic properties roughly match to those of R134a. The evaporation and condensation temperatures are 4.4 °C and 37.8 °C respectively and no superheat or subcooling was considered. Better predicted energy efficiency of DR-11 relative to HFO-1234yf possibly causes to be chosen over HFO-1234yf due to its performance benefits and its low flammability despite of its higher GWP. (Hughes et al., 2010)

Table 18. Predicted thermodynamic cycle performance of DR-11 and HFO-1234yf relative to R-134a. (Hughes et al., 2010)

(T_{eva}= 4.4° C, T_{cond}= 37.8 °C)

	DR-11 vs R-134a %	HFO-1234yf vs R-134a %
Compression ratio	-3.5	-5.8
Compressor enthalpy rise	-11.7	-19.1
Compressor discharge temperature [°C]	-9.8	-15.9
Net refrigeration effect per unit mass of refrigerant	-13.9	-22.8
Vapor density at compressor suction	17.8	21.2
Cooling capacity per unit volume of refrigerant	1.5	-6.5
COP $_{cooling}$	-2.5	-4.5

4.3.9 DR-2

DR-2 is another HFO-based low GWP refrigerant developed at Dupont Company and it's been offered to be a replacement for HCFC-123. Although its composition is undisclosed, it has GWP less than 10 while it is not an ozone depleting material. It is non-flammable and has negligible glide, desirable toxicity level. It can be a noticeable eco-friendly option for the low pressure and high energy efficiency centrifugal chillers. Since HCFC-123 is an ozone depleting substance, it is been planned to be phased out gradually according to the Montreal Protocol. DR-2 cannot be used as a drop-in replacement for HCFC-123. Table 19 shows great environmental properties of DR-2 in comparison to HCFC-123. Its atmospheric life time is quite acceptable.

Table 19. Thermodynamic properties of DR-2 and HCFC-123. (Kontomaris, 2010)

	DR-2	HCFC-123
Chemical formula	Undisclosed	$C_2HCl_2F_3$
Critical Pressure [kPa]	2.903	3.668
Critical Temperature [°C]	171.3	102
Normal Boiling Point [°C]	-33.4	-26
Safety Class	NA	B1
GWP	9.4	77
ODP	0	0.02
Atmospheric Life Time [year]	<0.0658 (24 day)	1.3
Lower Flammability Limit [vol.% in air-23°C]	-	-

Figure 7 illustrate the vapor pressure curves of DR-2 and HCFC-123. As can be seen DR-2 has slightly lower pressures than HCFC-123 in working temperatures range of 4.4-37.8 °C. (Kontomaris, 2010)
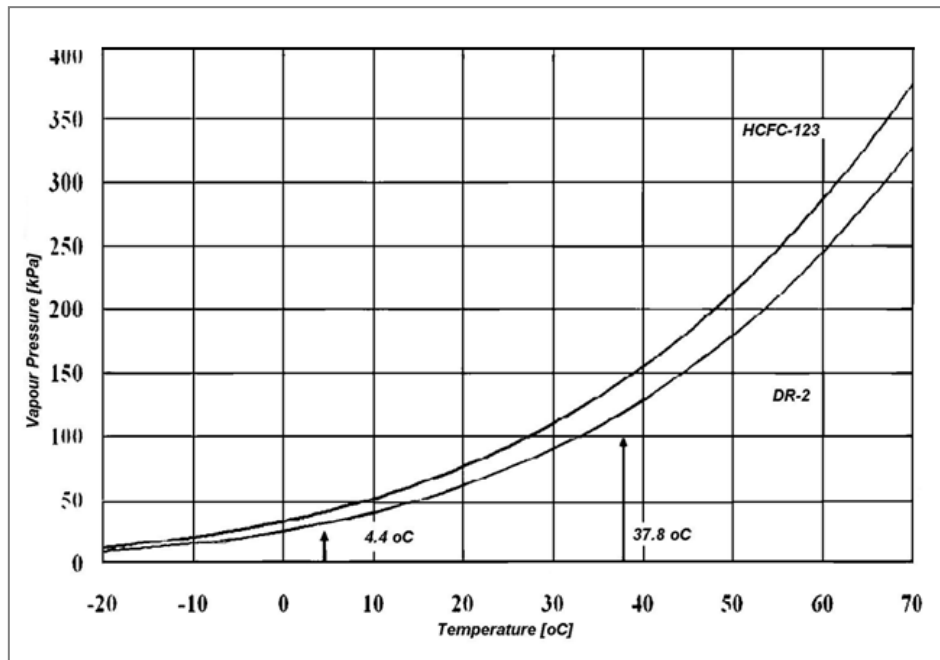
Figure 7.Vapour pressure diagram of DR-2 and HCFC-123. (Kontomaris, 2010)

In a chiller, cycle performance of DR-2 was predicted by Kontomaris through computational modeling. The condensing and evaporating temperature were kept respectively at 37.8°C and 4.4 °C with cooling load of 3.517 kW. Compressor Efficiency is 0.70 and there are no gas superheating, liquid subcooling and pressure drop in the heat exchangers.

Table 20. Predicted Thermodynamic Cycle Performance of DR-2 Relative to HCFC_123 (Kontomaris, 2010)

	HCFC-123	DR-2	DR-2 vs HCFC-123
Cooling Duty [kW]	3,517	3,517	
Compressor Enthalpy Rise –Isentropic [kJ/kg]	19.91	19.36	-2.7%
Compressor Enthalpy Rise –Actual [kJ/kg]	28.44	27.66	-2.7%
Compressor Discharge Temp [°C]	48.7	41.9	-6.8 °C
Evaporator Enthalpy Rise - Net Refrigeration [kJ/kg]	146.41	140.17	-4.3%
Coefficient of Performance - Isentropic	7.35	7.24	-1.6%
Coefficient of Performance - Actual	5.15	5.07	-1.6%
Vapor Density Compressor Inlet [Kg/m³]	2.68	2.21	-17.5%
Volumetric Cooling Capacity [kJ/m³]	392.68	310.23	-21%
Volumetric Flow Rate at Compressor Suction [m³/s]	8.96	11.34	26.6%

HCFC-123 is banned in most of developed countries including USA from 2010. The available replacements are DR-2, R-134a and HFO-1234yf. Table 20 shows DR-2 has lower COP and volumetric cooling capacity than those of HCFC-123. However, total cycle performance of DR-2 seems to be comparable to HCFC-123. Hughes and his colleagues have also claimed that COP of DR-2 is 4.6% higher than R-134a, 9.55 higher than HFO-1234yf and 7.2% greater than DR-11. (Hughes et al., 2010)

Its lower vapor pressure and higher energy efficiency relative to R-134a, in company with desirable environmental and safety characteristics make it a promising option in the near future in refrigeration industry. (Kontomaris, 2010)

4.4 Summary of the candidates refrigerants

Ecological concerns resulted by HFCs refrigerants have led to many international studies to decrease the harmful environmental impacts of exiting refrigerants. Researchers and companies are working towards developing new materials with less environmental effects. The refrigeration industry work hard to meet the requirements for the new environmental regulations. There are refrigerants which have low GWP and acceptable potential to substitute the common refrigerants. Natural refrigerants such as: carbon dioxide, ammonia and hydrocarbons, new refrigerants like HFO-1234yf and HFO-1234ze and blends of new refrigerants like DR-2 and DR-11 are candidates in this filed.

Flammability is the matter of discussion on new refrigerants. Thus more studies are being done to develop new blends so that they can overcome this problem as well.

5 Cycle performance calculations

This study continued by theoretical calculation of cycle performance of two new refrigerants R1234yf and R1234ze. Moreover, an experiment has been done in a vapor compression cycle test rig to compare the experimental cycle performance of R1234yf as the new refrigerant and R134a as the common one. To accomplish these, we have to use thermodynamic laws.

5.1 Fundamental concepts of the vapor compression cycle

Equation 1 expresses the heat balance over a vapor compression system. Q_1 is rejected heat from the cycle at higher temperature and Q_2 is the extracted heat at the lower temperature and E is the required work to lift the heat Q_2 from lower temperature to higher temperature. According to the first law of thermodynamic, the cycle work, transferred and rejected heat to the cycle are parameters that can be calculated by heat balance of the system.

$$Q_1 = Q_2 + E \quad (1)$$

The ratio of the refrigerating capacity to the power input to the compressor called coefficient of performance of the refrigeration cycle, COP, is one of the parameters in analyzing cycle performance.

$$COP_2 = \frac{Q_2}{E} \quad (2)$$

For a Carnot cycle the coefficient of performance for refrigeration is,

$$COP_{2C} = \frac{t_2}{t_1 - t_2} \quad (3)$$

In which t1 is condensing temperature and t2 is evaporating temperature in Kelvin. The isentropic Carnot efficiency also is,

$$\eta_{cd} = \frac{COP_{2d}}{COP_{2C}} \quad (4)$$

In which $COP_{2d} = \frac{Q_2}{E_d} = \frac{h_{2k} - h_s}{h_{1k,is} - h_{2k}} \quad (5)$

5.2 Evaporator Energy balance

Figure 8 shows the enthalpy-pressure diagram for a vapor compression cycle. Refrigeration effect and capacity of the cycle will be gained by heat balance over the evaporator. The refrigeration capacity is calculated by the enthalpy difference over the refrigerant side of the evaporator.

$Q_2 = \dot{m}.(h_{2k} - h_s)$ (6)

For evaluating the volumetric refrigerating effect, the volume flow rate at outlet of the evaporator is required.

$V_2 = \dot{m}v_{2k}$ (7)

$q_v = \dfrac{Q_2}{V_2} = \dfrac{h_{2k} - h_s}{v_{2k}}$ (8)

It is assumed the evaporator is working under an isobaric condition. In the test rig the evaporator inlet is a mixture of saturated gas and saturated liquid and the outlet gas is typically superheated 6-9 K.
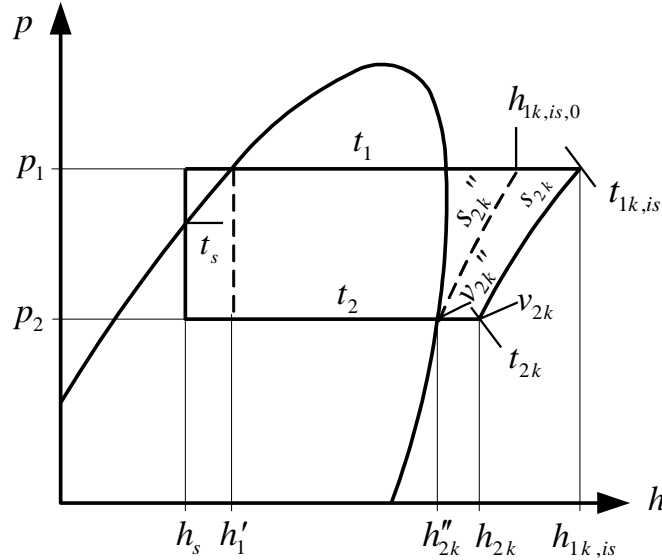
Figure 8.Pressure vs. Enthalpy diagram for a vapor compression cycle. (Granryd, 2005):

5.3   Compressor Energy balance

Superheated vapor enters to the compressor and its pressure and temperature increase. In an ideal condition compressor operates in isentropic state. The required work for isentropic compression is proportional to the enthalpy change during compression.

$E_d = \dot{m}(h_{1k,is} - h_{2k})$ (9)

and ε_d is also defined as $\varepsilon_d = (h_{1k,is} - h_{2k})$. With respect to the equation (9), volumetric compression work ε_v is equal to:

$\varepsilon_v = \dfrac{E_d}{V_2} = \dfrac{h_{1k,is} - h_{2k}}{v_{2k}}$ (10)

In actual operation, isentropic process is an ideal term which is hardly gained. The actual work should compensate fluid friction, mechanical friction and other losses inside the compressor, thus the actual compressor power is calculated when the actual enthalpy at the outlet of compressor, h_{1k}, is read at real pressure and temperature at the exit.

$E_k = \dot{m}(h_{1k} - h_{2k})$ (11)

E_k is the power input to the refrigerant while it is compressed.

Total isentropic compression efficiency is defined as η_k .

$$\eta_k = \frac{E_d}{E_k} \quad (12)$$

For a positive displacement compressor the volume flow rate at the inlet is always smaller than the theoretical swept volume flow. Swept flow, V_s, can be defined as the possible inlet vapor volume flow to the compressor. Volumetric efficiency is used to explain this,

$$\eta_s = \frac{V_{in}}{V_s} \quad (13)$$

5.4   Condenser Energy balance

Hot high pressure gas enters to the condenser and is changed to the liquid in an isobaric condition. The amount of rejected heat is calculated by enthalpy rate changes in refrigerant side of the condenser.

$$Q_1 = \dot{m}(h_{1k} - h_s) \quad (14)$$

The refrigerant at exit of the condenser is about typically 4-8 K subcooled.

6   Basic cycle data

Basic cycle data for the new refrigerants R1234yf and R1234ze have been calculated by means of RefProp 7.01 for the cycle shown by its P-h diagram in figure 8. Different characteristics of basic vapor compression cycles such as volumetric cooling capacity, isentropic compression work, COP and cycle Carnot efficiency have been evaluated for systems with no liquid sub cooling or gas superheating at various condensing and evaporating temperatures.

Influence of superheating and subcooling of the working fluid on the calculated COP and volumetric cooling capacity can be determined by y-factors. The y-factors illustrate the relative change of COP and cooling capacity per degree of superheating and subcooling compared to the basic cycle data with no superheating and subcooling of the refrigerant. They can be defined as follows (Granryd, 2005):

y_1 indicates relative change in COP_{2d} and volumetric cooling capacity due to liquid sub cooling formed at condenser :

$$y_1 = (\frac{h''_{2k} - h_s}{h''_{2k} - h'_1} - 1) \cdot \frac{100}{t_1 - t_s} \quad (15)$$

In which t_s is temperature of the refrigerant when it goes out from the condenser and h_s is the corresponding enthalpy at this point. Furthermore, h''_{2k} is enthalpy of saturated gas at evaporating temperature and h'_1 is enthalpy of saturated liquid at condensing temperature. Increasing the subcooling of refrigerant in the condenser influences the refrigerating effect. As figure 8 shows, when the amount of subcooling increases, enthalpy of refrigerant at condenser outlet (h_s) decreases. Consequently refrigerating effect which is proportional to $h_{2k} - h_s$, increases. This growth in refrigerating effect doesn't affect compression work. However, increasing the refrigerating effect leads to increase COP_{2d} of the cycle as well.

y_2 illustrates relative change in volumetric cooling capacity caused by internal gas superheating, formed at evaporator:

$$y_2 = (\frac{h_{2k} - h'_1}{v_{2k}} \cdot \frac{v''_{2k}}{h''_{2k} - h'_1} - 1) \cdot \frac{100}{t_{2k} - t_2} \quad (16)$$

In which h_{2k} is enthalpy of refrigerant when it goes out from the evaporator, v''_{2k} is specific volume of saturated liquid at evaporating temperature and v_{2k} is the specific volume at the evaporator outlet and t_{2k} is temperature of the refrigerant at evaporator outlet. Increasing the superheating of the refrigerant at

evaporator actually enhances the value of h_{2k}, so $h_{2k} - h_{2k}''$ which is proportional to refrigerating effect increases. However, specific volume develops from v_{2k}'' to v_{2k}. Thus y_2 can be negative or positive.

Moreover y_3 evaluates effect of internal superheating in COP_{2d}:

$$y_3 = \left(\frac{h_{2k} - h_1'}{h_{1k,is} - h_{2k}} \cdot \frac{h_{1k,is,0} - h_{2k}''}{h_{2k}'' - h_1'} - 1\right) \cdot \frac{100}{t_{2k} - t_2} \qquad (17)$$

$h_{1k,is}$ is the enthalpy at compressor outlet for an isentropic compression and $h_{1k,is,0}$.is the enthalpy at compressor outlet for an isentropic compression and no superheating in the evaporator. Increasing internal superheating enhances both refrigerating effect and compression work. Since the volumetric compression work can be defined as $\varepsilon_v = \frac{q_v}{COP_{2d}}$, so increase in volumetric compression work is about y_2-y_3.

y_4 indicates relative change in COP_{2d} caused by external gas superheating (due to outside refrigerated space impacts):

$$y_4 = \left(\frac{h_{1k,is,0} - h_{2k}''}{h_{1k,is} - h_{2k}} - 1\right) \cdot \frac{100}{t_{2k} - t_2} \qquad (18)$$

y_4 is always negative and it has small value. Since the volumetric refrigeration effect can be rewritten as $q_v = \varepsilon_v . COP_{2d}$, the increase in q_v compared to the basic cycle can be obtained by y_2-y_3+y_4.

Tables 21 and 22 demonstrate the basic cycle data for R1234yf and R1234ze. Evaluation of the tables indicate that R1234ze has higher pressure ratio and lower compressor discharge temperature than those of R134a and also its COP and isentropic Carnot efficiency are less in many points. Higher pressure ratio means higher compressing energy consumption which leads to decrease in the COP of the system. R1234yf has lower pressure ratio and discharge pressure than R134a but it has lower COP and isentropic Carnot efficiency. From table 20 and 21 it can be concluded that systems working with R1234ze as refrigerant need larger compressors for a given cooling capacity to be obtained. On the other hand lower condensing energy is produced by using R1234yz in the systems with the same condensing and evaporating temperatures. Figure 9 and 10 compare volumetric cooling capacity and isentropic Carnot efficiency of R1234yf, R1234ze and R134a. While at lower temperatures R1234yf has lower isentropic efficiency, by increasing the temperature, isentropic efficiency of all three refrigerants get closer to each other. As it can be seen in figure 10 R1234yf and R134a have close volumetric cooling capacities at different evaporating and condensing temperatures but R1234ze has lowest value at each point.
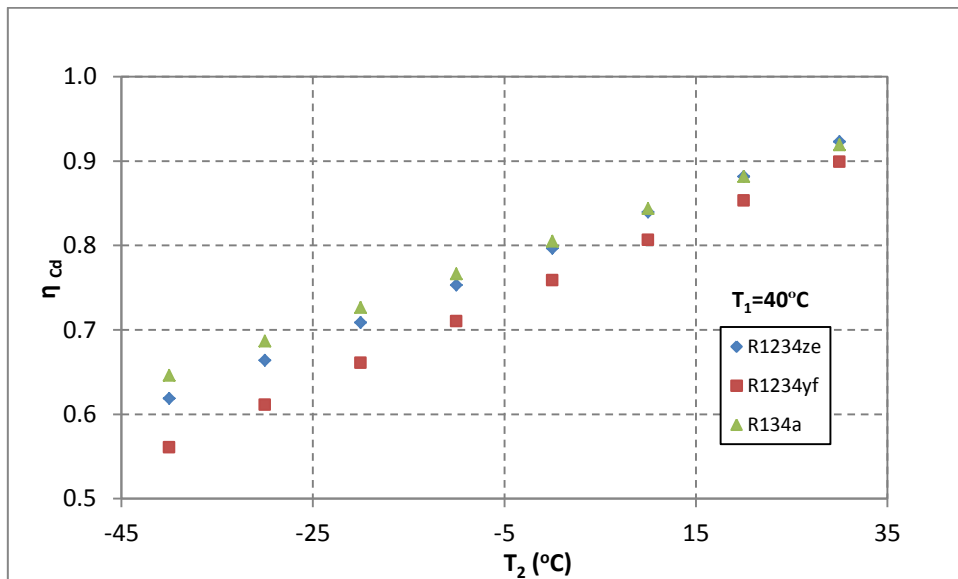

Figure 9.Isentropic Carnot efficiency at different evaporating temperatures and constant condensing temperature of 40ºC.
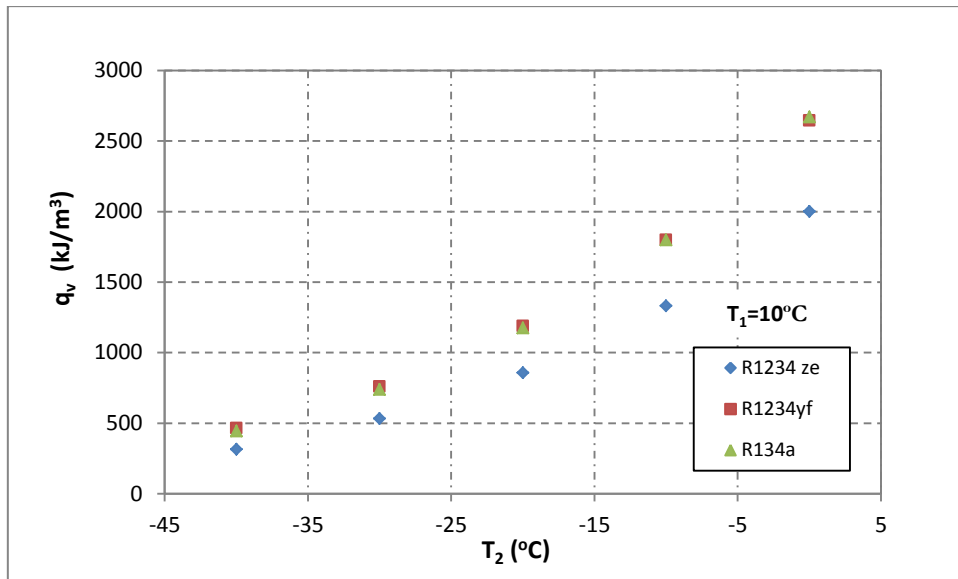
Figure 10.Volumetric cooling capacity at different evaporating temperatures and constant condensing temperature of 10ºC.

Table 21. Cycle data for R1234yf

T$_1$ (°C)	T$_2$(°C)	P1 (bar)	P2(bar)	P1/P2	T$_{1k\_is}$	q$_v$	ε$_v$	COP $_{2D}$	COP $_{2C}$	η $_{Cd}$	y$_1$	y$_2$	y$_3$	y$_4$
R1234yf														
-20	**-50**	1,51	0,376	4,024	-17,3192	363,8	55,2	6,59	7,43	0,887	0,805	0,019	0,022	-0,469
-20	**-40**	1,51	0,626	2,416	-18,9164	612,6	56,9	10,76	11,65	0,923	0,770	0,020	0,018	-0,470
-20	**-30**	1,51	0,993	1,523	-19,7591	985,7	42,3	23,30	24,30	0,959	0,738	0,016	0,014	-0,472
-10	**-50**	2,22	0,376	5,910	-7,55922	334,0	71,3	4,68	5,58	0,840	0,899	0,062	0,063	-0,471
-10	**-40**	2,22	0,626	3,549	-9,15179	564,5	82,7	6,83	7,77	0,879	0,857	0,061	0,056	-0,473
-10	**-30**	2,22	0,993	2,236	-9,99168	911,6	81,8	11,14	12,15	0,917	0,818	0,056	0,049	-0,476
-10	**-20**	2,22	1,512	1,469	-10	1416,1	58,7	24,14	25,30	0,954	0,783	0,047	0,041	-0,481
0	**-40**	3,16	0,626	5,051	0,254453	515,3	106,7	4,83	5,83	0,829	0,963	0,112	0,101	-0,478
0	**-30**	3,16	0,993	3,183	6,31E-12	835,7	118,6	7,04	8,10	0,870	0,916	0,104	0,089	-0,483
0	**-20**	3,16	1,512	2,090	6,31E-12	1303,1	113,3	11,50	12,65	0,909	0,873	0,092	0,077	-0,491
0	**-10**	3,16	2,221	1,423	6,31E-12	1965,2	78,8	24,93	26,30	0,948	0,834	0,076	0,065	-0,499
10	**-40**	4,38	0,626	6,995	10	464,7	128,9	3,60	4,66	0,773	1,098	0,175	0,157	-0,486
10	**-30**	4,38	0,993	4,407	10	757,7	152,8	4,96	6,08	0,816	1,038	0,163	0,137	-0,493
10	**-20**	4,38	1,512	2,895	10	1187,2	164,0	7,24	8,43	0,858	0,985	0,147	0,119	-0,503
10	**-10**	4,38	2,221	1,971	10	1798,1	152,0	11,83	13,15	0,900	0,937	0,128	0,102	-0,514
10	**0**	4,38	3,161	1,385	10	2645,6	103,1	25,66	27,30	0,940	0,894	0,105	0,087	-0,526
20	**-40**	5,92	0,626	9,458	20	412,6	149,5	2,76	3,88	0,711	1,272	0,256	0,227	-0,496
20	**-30**	5,92	0,993	5,959	20	677,4	184,4	3,67	4,86	0,756	1,194	0,237	0,197	-0,508
20	**-20**	5,92	1,512	3,914	20	1067,9	210,9	5,06	6,33	0,801	1,126	0,217	0,170	-0,520
20	**-10**	5,92	2,221	2,665	20	1626,2	219,6	7,40	8,77	0,845	1,066	0,194	0,147	-0,534
20	**0**	5,92	3,161	1,872	20	2404,2	198,4	12,12	13,65	0,888	1,012	0,167	0,127	-0,547
20	**10**	5,92	4,377	1,352	20	3466,4	131,8	26,31	28,30	0,930	0,965	0,134	0,109	-0,562

T₁ (°C)	T₂(°C)	P1 (bar)	P2(bar)	P1/P2	T₁ₖ_ᵢₛ	qᵥ	εᵥ	COP₂D	COP₂C	η Cd	y₁	y₂	y₃	y₄
30	-40	7,84	0,626	12,521	30	358,9	168,5	2,13	3,33	0,640	1,508	0,364	0,320	-0,511
30	-30	7,84	0,993	7,889	30	594,7	213,4	2,79	4,05	0,688	1,404	0,336	0,277	-0,525
30	-20	7,84	1,512	5,182	30	944,9	254,0	3,72	5,06	0,735	1,313	0,307	0,239	-0,541
30	-10	7,84	2,221	3,528	30	1448,9	281,9	5,14	6,58	0,782	1,234	0,277	0,206	-0,557
30	0	7,84	3,161	2,479	30	2155,3	286,2	7,53	9,10	0,828	1,165	0,245	0,178	-0,573
30	10	7,84	4,377	1,790	30	3124,3	253,1	12,34	14,15	0,872	1,105	0,208	0,153	-0,590
30	20	7,84	5,918	1,324	30	4431,5	165,0	26,85	29,30	0,916	1,052	0,164	0,131	-0,611
40	-40	10,18	0,626	16,273	40	303,4	185,8	1,63	2,91	0,561	1,849	0,516	0,453	-0,528
40	-30	10,18	0,993	10,253	40	509,1	240,0	2,12	3,47	0,611	1,699	0,471	0,390	-0,546
40	-20	10,18	1,512	6,734	40	817,7	293,4	2,79	4,22	0,661	1,572	0,429	0,336	-0,564
40	-10	10,18	2,221	4,585	40	1265,6	338,8	3,74	5,26	0,710	1,464	0,388	0,289	-0,583
40	0	10,18	3,161	3,222	40	1897,8	366,6	5,18	6,83	0,759	1,371	0,347	0,249	-0,602
40	10	10,18	4,377	2,326	40	2770,4	364,3	7,61	9,43	0,806	1,291	0,303	0,215	-0,622
40	20	10,18	5,918	1,721	40	3953,4	316,3	12,50	14,65	0,853	1,222	0,254	0,185	-0,646
40	30	10,18	7,835	1,300	40	5536,1	203,2	27,24	30,30	0,899	1,163	0,196	0,156	-0,678
50	-40	13,02	0,626	20,808	50	245,7	201,6	1,22	2,59	0,471	2,387	0,748	0,663	-0,548
50	-30	13,02	0,993	13,110	50	420,1	264,2	1,59	3,04	0,523	2,145	7007,916	1556,343	-938,568
50	-20	13,02	1,512	8,611	50	685,5	329,3	2,08	3,61	0,576	1,954	0,603	0,483	-0,590
50	-10	13,02	2,221	5,863	50	1075,0	390,7	2,75	4,38	0,628	1,795	0,543	0,415	-0,611
50	0	13,02	3,161	4,119	50	1630,2	439,7	3,71	5,46	0,679	1,663	0,487	0,357	-0,632
50	10	13,02	4,377	2,975	50	2402,5	465,5	5,16	7,08	0,729	1,551	0,432	0,308	-0,656
50	20	13,02	5,918	2,200	50	3456,3	454,2	7,61	9,77	0,779	1,456	0,374	0,265	-0,684
50	30	13,02	7,835	1,662	50	4873,6	388,5	12,54	15,15	0,828	1,377	0,310	0,225	-0,721
50	40	13,02	10,183	1,279	50	6760,9	246,5	27,42	31,30	0,876	1,310	33,163	29,141	-41,078

Table 21.Cycle data for R1234ze

T_1 (°C)	T_2(°C)	P1 (bar)	P2(bar)	P1/P2	T_{1k_is}	q_v	ε_v	COP $_{2D}$	COP $_{2C}$	η_{Cd}	y_1	y_2	y_3	y_4
							R1234ze							
-20	-60	0,968	0,112	8,632	-9,922	122,1	26,7	4,58	5,33	0,86	0,753	-0,047	-0,028	-0,454
-20	-50	0,968	0,210	4,619	-13,971	228,2	34,3	6,66	7,43	0,90	0,723	-0,038	-0,028	-0,451
-20	-40	0,968	0,368	2,634	-16,860	401,5	37,0	10,85	11,65	0,93	0,695	-0,032	-0,028	-0,449
-20	-30	0,968	0,611	1,585	-18,810	670,7	28,6	23,43	24,30	0,96	0,669	-0,029	-0,029	-0,448
-10	-50	1,474	0,210	7,031	-3,381	211,5	44,4	4,77	5,58	0,86	0,796	-0,004	0,006	-0,450
-10	-40	1,474	0,368	4,008	-6,277	373,2	53,9	6,92	7,77	0,89	0,763	0,000	0,003	-0,449
-10	-30	1,474	0,611	2,413	-8,231	625,2	55,5	11,26	12,15	0,93	0,732	0,001	0,001	-0,449
-10	-20	1,474	0,968	1,522	-9,423	1002,2	41,2	24,31	25,30	0,96	0,704	-0,001	-0,003	-0,451
0	-40	2,165	0,368	5,888	3,801	344,3	69,7	4,94	5,83	0,85	0,844	0,038	0,040	-0,451
0	-30	2,165	0,611	3,544	1,850	578,7	80,7	7,17	8,10	0,89	0,808	0,038	0,034	-0,452
0	-20	2,165	0,968	2,236	0,661	930,6	79,8	11,66	12,65	0,92	0,774	0,034	0,028	-0,455
0	-10	2,165	1,474	1,469	0,086	1440,4	57,2	25,16	26,30	0,96	0,743	0,026	0,022	-0,459
10	-40	3,083	0,368	8,386	13,482	314,7	84,5	3,73	4,66	0,80	0,945	0,084	0,083	-0,454
10	-30	3,083	0,611	5,048	11,543	531,2	104,3	5,09	6,08	0,84	0,900	0,081	0,073	-0,456
10	-20	3,083	0,968	3,184	10,362	857,4	115,9	7,40	8,43	0,88	0,860	0,075	0,064	-0,460
10	-10	3,083	1,474	2,092	10,000	1331,5	110,7	12,02	13,15	0,91	0,823	0,066	0,055	-0,466
10	0	3,083	2,165	1,424	10,000	2000,9	77,1	25,96	27,30	0,95	0,789	0,053	0,045	-0,474
20	-40	4,273	0,368	11,624	22,872	284,5	98,3	2,89	3,88	0,75	1,069	0,141	0,135	-0,458
20	-30	4,273	0,611	6,997	20,954	482,6	126,2	3,82	4,86	0,79	1,014	0,134	0,121	-0,462
20	-20	4,273	0,968	4,414	20,000	782,4	149,6	5,23	6,33	0,83	0,964	0,125	0,107	-0,467
20	-10	4,273	1,474	2,900	20,000	1220,1	160,6	7,60	8,77	0,87	0,919	0,113	0,093	-0,475
20	0	4,273	2,165	1,974	20,000	1840,3	148,9	12,36	13,65	0,91	0,878	0,098	0,079	-0,485

T₁ (°C)	T₂(°C)	P1 (bar)	P2(bar)	P1/P2	T₁k_is	qᵥ	εᵥ	COP 2D	COP 2C	η Cd	y₁	y₂	y₃	y₄
20	**10**	4,273	3,083	1,386	20,000	2697,7	101,0	26,71	28,30	0,94	0,841	0,079	0,066	-0,496
T₁ (°C)	**T₂(°C)**	**P1 (bar)**	**P2(bar)**	**P1/P2**	**T₁k_is**	**qᵥ**	**εᵥ**	**COP 2D**	**COP 2C**	**η Cd**	**y₁**	**y₂**	**y₃**	**y₄**
30	**-40**	5,784	0,368	15,733	32,080	253,4	111,1	2,28	3,33	0,69	1,231	0,214	0,201	-0,464
30	**-30**	5,784	0,611	9,470	30,193	432,7	146,6	2,95	4,05	0,73	1,159	0,202	0,180	-0,469
30	**-20**	5,784	0,968	5,974	30,000	705,5	180,8	3,90	5,06	0,77	1,096	0,188	0,160	-0,476
30	**-10**	5,784	1,474	3,925	30,000	1105,8	206,8	5,35	6,58	0,81	1,039	0,172	0,139	-0,487
30	**0**	5,784	2,165	2,672	30,000	1675,6	215,5	7,78	9,10	0,85	0,989	0,154	0,120	-0,499
30	**10**	5,784	3,083	1,876	30,000	2466,3	194,8	12,66	14,15	0,89	0,943	0,132	0,102	-0,513
30	**20**	5,784	4,273	1,354	30,000	3541,3	129,3	27,39	29,30	0,93	0,903	0,105	0,087	-0,527
40	**-40**	7,666	0,368	20,853	41,224	221,6	122,9	1,80	2,91	0,62	1,448	0,310	0,289	-0,472
40	**-30**	7,666	0,611	12,552	40,000	381,4	165,5	2,30	3,47	0,66	1,353	0,289	0,258	-0,479
40	**-20**	7,666	0,968	7,918	40,000	626,5	209,7	2,99	4,22	0,71	1,269	0,268	0,227	-0,489
40	**-10**	7,666	1,474	5,203	40,000	988,3	249,6	3,96	5,26	0,75	1,196	0,247	0,198	-0,502
40	**0**	7,666	2,165	3,542	40,000	1506,2	277,1	5,44	6,83	0,80	1,131	0,223	0,171	-0,517
40	**10**	7,666	3,083	2,487	40,000	2228,4	281,5	7,92	9,43	0,84	1,074	0,198	0,147	-0,532
40	**20**	7,666	4,273	1,794	40,000	3214,4	248,9	12,91	14,65	0,88	1,023	0,168	0,126	-0,549
40	**30**	7,666	5,784	1,325	40,000	4538,1	162,3	27,97	30,30	0,92	0,978	0,132	0,107	-0,569
50	**-40**	9,975	0,368	27,133	50,443	188,7	133,9	1,41	2,59	0,54	1,758	0,442	0,411	-0,482
50	**-30**	9,975	0,611	16,332	50,000	328,5	182,9	1,80	3,04	0,59	1,620	0,408	0,363	-0,491
50	**-20**	9,975	0,968	10,303	50,000	544,9	236,3	2,31	3,61	0,64	1,505	0,376	0,318	-0,505
50	**-10**	9,975	1,474	6,770	50,000	867,1	289,0	3,00	4,38	0,68	1,406	0,345	0,277	-0,520
50	**0**	9,975	2,165	4,608	50,000	1331,5	333,8	3,99	5,46	0,73	1,320	0,314	0,240	-0,537
50	**10**	9,975	3,083	3,236	50,000	1983,1	361,3	5,49	7,08	0,78	1,245	0,282	0,208	-0,555
50	**20**	9,975	4,273	2,334	50,000	2877,1	359,1	8,01	9,77	0,82	1,179	0,247	0,179	-0,575
50	**30**	9,975	5,784	1,725	50,000	4082,7	311,8	13,09	15,15	0,86	1,122	0,208	0,153	-0,598
50	**40**	9,975	7,666	1,301	50,000	5686,8	200,2	28,41	31,30	0,91	1,072	0,160	0,127	-0,626

The tables show that R1234ze has higher pressure ratio than R1234yf and R134a. Cycle data for R134a can be seen in (Granryd et al., 2005). It can be seen from the table 20 and 21 that for example at t_1=20ºC and t_2=-10ºC, R1234ze and R1234yf have respectively 26% and 1.9% lower volumetric cooling capacity than R134a. Although at the same thermal condition COP of R134a is just about 0.6% higher than R 1234ze and 3.2% higher than that of R1234yf, the common refrigerant has higher isentropic Carnot efficiency by 1% and 3% respectively for R1234ze and R1234yf.

As stated, numbers given in the tables are used for basic cycles. In practice there is mostly also a certain subcooling of liquid before the expansion valve along with superheat of vapor before the compressor. Tables also show both new refrigerants are more influenced by vapor superheating and liquid subcooling than the common refrigerant, R134a. In all of the condensing temperatures one degree subcooling increases COP and cooling capacity of R1234yf and R1234ze more than those of R134a. For instance in table 20 and 21 can be seen that at t_1=20ºC and t_2=-10ºC, R1234yf has y_1=1.066, y_2=0.194 and y_3=0.147 which mean one degree Celsius subcooling in the condenser increase COP_{2d} and q_v of the system by 1.066% and also one degree Celsius superheating raises q_v, COP_{2d} and ε_v by 0.194%, 0.147% and 0.047% respectively. It is worthwhile to mention that subcooling of refrigerant doesn't effect on compression work. However, superheating of refrigerant in the evaporator increase the compression work, ε_v, about y_2-y_3 which is usually small. Similarly at t_1=20ºC and t_2=-10ºC, R134a (See Granryd, et al., 2005) has y_1=0.846, y_2=0.02 and y_3=0.003 that illustrate one degree Celsius subcooling of refrigerant in the condenser can enhance the COP_{2d} and q_v of the cycle by 0.846% and also one degree superheating of refrigerant in the evaporator increases the q_v, COP_{2d} and ε_v by 0.02%, 0.003%, 0.017% respectively.

Comparing refrigerants, y_1, y_2 and y_3 for R1234yf at t_1=20ºC and t_2=-10ºC are higher than R134a by 25%, 975% and 36% respectively. Hence for increasing one degree subcooling of the refrigerant at the condenser, the COP_{2d} and q_v of R1234yf are influenced 25% more than R134a. It means one degree subcooling of refrigerant influences COP_{2d} and q_v of R1234yf about 25% more compared to one degree subcooling of R134a. Similarly, one degree superheating of refrigerant has about 975% higher effect on q_v of R1234yf rather than that for R134a. It is worthwhile to mention that it is still a small value.

Moreover, at t_1=20ºC and t_2=-10ºC, R1234ze has y_1=0.919, y_2=0.113 and y_3=0.093 which demonstrate one degree centigrade subcooling of liquid increase q_v and COP_{2d} by 0.919%, while one degree centigrade superheating of vapor increases q_v, COP_{2d} and ε_v respectively by 0.113%, 0.093% and 0.02%. Comparing to R134a, it can be concluded that R1234yz has higher y_1 and y_2 by 8% and 595% respectively.

As equation 15 indicates for calculations of y_1 the amount of t_1-t_s (degree of subcooling) used in the calculation, influences the value of y_1. Likewise y_2 is affected by the amount of superheating in equation 16 it is shown by t_{2k}-t_2. Here the effects of different t_1-t_s and t_{2k}-t_2 on the value of y_1 and y_2 respectively have been investigated. On the other hand different liquid subcooling and gas superheating temperatures were applied. Thus the y_1 and y_2 for the R1234yf with different liquid subcooling and vapor superheating estimated temperatures have been evaluated at condensing temperature of 20ºC. In figure 11 t_1-t_s have been chosen as 3, 4, 5, and 6 K and the y_1 factor for R1234yf has been calculated by means of equation 15. This is, liquid subcooling temperatures were assumed 3-6 K, while condenser is working at constant temperatures of 20ºC and evaporating temperature range is -40-10ºC.
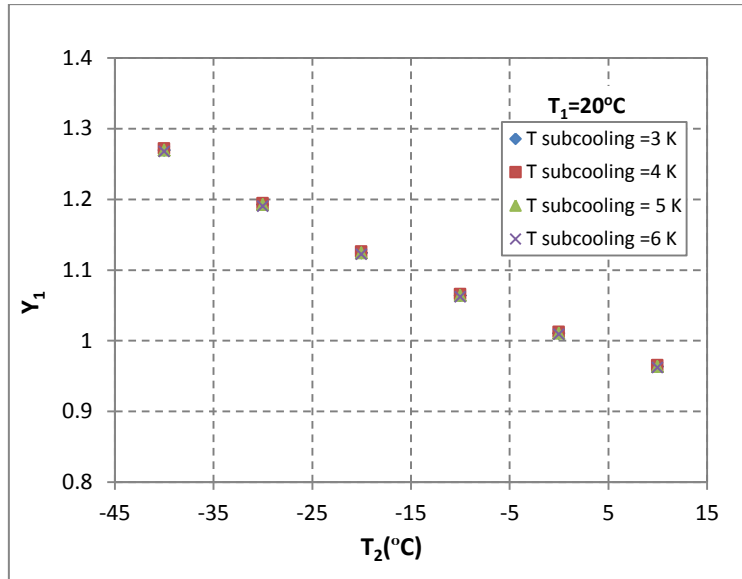
Figure 11.Effect of different amount of liquid subcooling on calculation of y_1 at different evaporating temperatures and constant condensing temperature of 20ºC for R1234yf**.**

As figure 11 indicates the differences between calculated y_1 were very small. Similarly, y_2 also were calculated at different vapor superheating temperature (t_{2k}-t_2) assumed from 5-10 K and very small differences were observed between y_2 values at each point. As it is clear from figures 11 and 12 the deviations in y-factors at different temperatures are about 0.1202-0.01206% which can be considered negligible. So it can be concluded that the amount of t_{2k}-t_2 and t_1-t_s applied for calculation of y-factors don't make a noticeable difference in y-factor values.
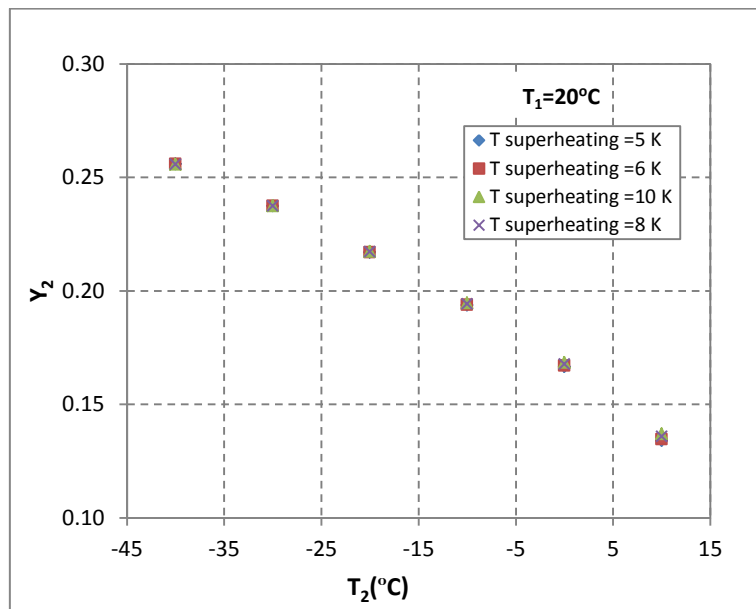

Figure 12.Effect of different amount of gas superheating on calculation of y_2 at different evaporating temperatures and constant condensing temperature of 20ºC for R1234yf.

7   Experimental part

The next part of this study includes an experiment in a vapor compression cycle. Cycle performance of two refrigerants, R1234yf and R134a are investigated at ten different cooling capacities from 1 kW to 3.2

kW and two constant condensing temperatures of 30ºC and 40ºC. Moreover, as the final phase of the project, heat transport behaviors of two refrigerants in the evaporator are evaluated. To reach this aim, from the experimental values the heat transfer coefficients of two refrigerants are calculated and finally the results are compared to a suitable heat transfer correlation from the literature.

7.1   Experimental set up

The test rig which has been used for analyzing R134a and R1234yf cycle performances consists of one refrigerant loop and one brine loop. Indeed it is made of basic components of any small vapor compression system. As can be seen in figure 13, in the refrigerant loop, working fluid passed from thermostatic expansion valve and then enters to the evaporator. Throughout the evaporator it absorbs heat from the brine side of the heat exchanger and is vaporized. Then the superheated refrigerant is compressed by the compressor and delivered to the discharge section. This high pressure and temperature vapor goes into the condenser and liquefies. The condensing heat is taken out by water serving as the heat sink in the other side of the heat exchanger. Just after the condenser there is a Coriolis flow meter in order to measure the flow rate of refrigerant in the system. Table 22 indicates all the existing parts of the test rig.
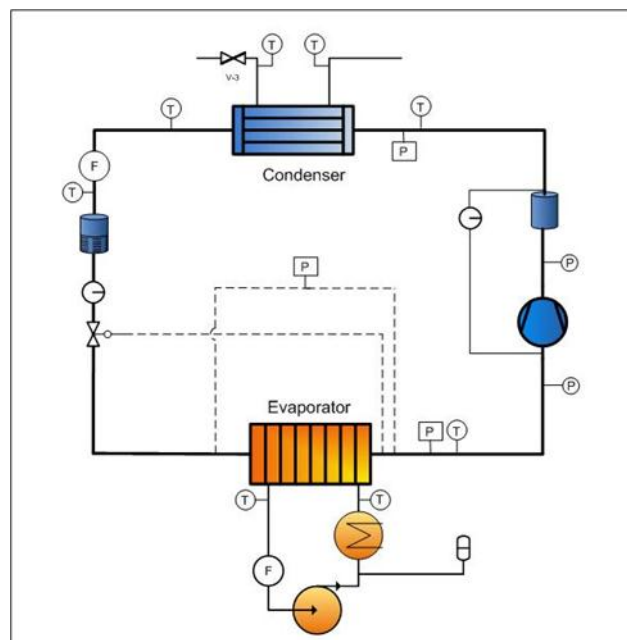

Figure 13.Schematic view of the test rig.

There is a brine loop which acts as the heat source of the cycle, the warm brine enters to the evaporator and provides the heat needed to vaporize the refrigerant flowing at the other side of the evaporator. The brine circuit includes a pump and an electrical heater provides the refrigerating effect for the cycle. Brine flow rate remains constant during the test. The brine as the secondary refrigerant is an aqueous solution made of ethylene glycol 26 wt% which its temperatures are affected by the evaporation temperature, speed of the pump and the amount of supplied heat from the electrical heaters.

Table 22.Test rig components

Symbol	Name	Model	Description
	Condensor	SWEP B10-20	Plate Heat Exchanger
	Liquid Dryer		
	Oil Seperator		
	Compressor	Mitsubishi R8 154VAC	Rolling Piston Type Rotary
	Evaporator	SWEP B10-10	Plate Heat Exchanger
	Heater		
	Pump	Grundfos A4 25-6U/130	
	Expansion Valve	Danfoss TEN 2	Thermostatic Expansion Valve
	Regulation Valve	Danfoss WVFX 10-25	
	Expansion Vessel		
	Sight Glass		
	Flow Meter	Micron Motion DS0125	Coriolis Mass Flow Meter
	Temperature Probe		
	Manometer		
	Pressure Tap		

7.2 Test procedure

Cooling capacity is evaluated at ten different heat loads supplied by the electrical heaters from 1kW to 3.2 kW and at two constant condensing temperatures of 30C and 40°C. Both condenser and evaporator are plate heat exchangers in which the condenser has 20 plates and evaporator has 10 plates. Each plate has 0.031 (m²) surface areas. The Compressor is rolling piston type. Specifications for the compressor and heat exchangers are available at appendix.

Temperatures are measured by nine thermocouples located in different sections of the system; four thermocouples record inlet and outlet temperatures of the hot and cold streams into the condenser, two thermocouples measure the temperatures of the brine which enters and exits to the evaporator and also one is located after the evaporator to measure the temperature of superheated refrigerant. One thermocouple also has been placed after the flow meter to indicate the temperature of the refrigerant before the expansion valve. Two pressure transducers and one differential pressure transducer have been used in the test rig to evaluate the pressures in both evaporator and condenser and also for measuring the pressure drop inside the evaporator. Manometers also have been located before and after the compressor. The data is sent to the logger and can be observed by means of a data collection program (VEE) in the computer. In order to minimize the ambient losses, the whole system has been isolated.

There are different methods to measure the cooling capacity and cycle performance of the refrigeration system. One way is to use mass flow rate of the refrigerant and the enthalpy difference over the evaporator. The enthalpy difference corresponding to the pressure and temperatures of inlet and outlet of the evaporator multiplied by mass flow rate, gives the cooling capacity of the system. The enthalpy of each condition has been gained by means of a refrigeration property computer program called RefProp 7.01.

Table 23 and 24 show the test condition of two studied refrigerants at the same heat load of the electrical heater and condensing temperature as a sample that can help to compare thermodynamic performance of two cycles.

Table 23.Experimental data at evaporator for both R1234yf and R134a (T_1=30°C).

Evaporator		
Primary side	R1234yf	R134a
Secondary side	Ethylene Glycol – Water 25.96%	Ethylene Glycol – Water 25.96%
Heat Load, Q_2(kW)	0.915	0.923
Evaporation temperature,T_2 (°C)	-12.90	-10.99
Outlet temperature(°C)	-4.295	-3.036
Evaporation Pressure (bar)	1.992	1.928
Refrigerant mass flow rate(g/s)	6.713	5.350
Pressure drop(bar)	0.020	0.018
Brine temperature change over the evaporator (K)	3.72	3.859

Table 24 .Experimental data at condenser for both R1234yf and R134a (T_1=30°C).

Condenser		
Primary side	R1234yf	R134a
Secondary side	Water	Water
Heat Load, Q_2 (kW)	0.915	0.923
Rejected heat from the condenser, Q_1(kW)	1.27	1.24
Condensing temperature,T_1 (°C)	29.736	29.494
Inlet temperature of refrigerant (°C)	59.957	73.24
Outlet temperature of refrigerant (°C)	19.174	18,745
Condensing pressure(bar)	7.779	7.591
Water temperature change over the condenser (K)	14.406	16.217

8   Heat transfer in a plate heat exchanger

There are two plate heat exchangers in the test rig, operating as the condenser and evaporator. The calculated refrigerant heat transfer coefficient is an experimental value and can be compared with the exiting correlations in the literature. In case of studying evaporation in the heat exchanger, the state of the refrigerant at inlet of the evaporator is important to analyze the heat transfer and pressure drop inside the test rig correctly.

8.1 Single phase flow inside the evaporator

The film heat transfer coefficient in a plate heat exchanger has been considered by many researchers. Most of them used a modified Dittus-Boelter type of equation with different exponents and constants. In most of the correlations geometry of plates are specific but some of the correlations like Coulson and Richardson and Wanniarachchi et al. can be used when geometry of the plates are unknown or limited information is available. (Ayub, 2003)

8.1.1 Wanniarachchi et al. correlation (1995)

It is a correlation developed by the year 1995 for laminar single phase flow. Chevron angle is necessary for calculation of the heat transfer and friction factor.

$$N_u = (Nu_1^3 + Nu_t^3)^{(1/3)}Pr^{(1/3)}(\frac{\mu}{\mu_w})^{0.17} \quad , \qquad 1 \le Re \le 104 \text{ , Herringbone plates} \qquad (19)$$

$$Nu_1 = 3.65(\beta)^{-0.455}(\phi)^{0.661}Re^{0.339} \quad \begin{cases} 20° \le \beta \le 60° \\ \beta > 62° \rightarrow \beta = 62° \end{cases} \qquad (20)$$

$$Nu_t = 12.6(\beta)^{-1.142}(\phi)^{1-m}Re^m \qquad (21)$$

$$m = 0.646 + 0.0011(\beta) \qquad (22)$$

$$f = (f_1^3 + f_t^3)^{1/3} \qquad (23)$$

$$f_1 = 1774\beta^{-1.026} \phi^2 Re^{-1} \qquad (24)$$

$$f_t = 46.6(\beta)^{-1.08}(\phi)^{(1+p)}Re^{-p} \qquad (25)$$

$$p = 0.00423(\beta) + 0.0000223(\beta)^2 \qquad (26)$$

In which β is chevron angle, Φ is enlargement factor, f is friction factor, p is a constant related to chevron angle for calculating friction factor. The Wanniarachchi correlation is highly depended to the geometry of the plate and is applicable when the plate characteristics are known and Reynolds number is not more than 104. It is worthwhile to mention that here in the experiment Reynolds number was 120- 600.

8.1.2 Talik et al. correlation

Talik et al. have derived a correlation to predict heat transfer coefficient and friction factor for water solution in a plate heat exchanger with following characteristics and condition. (Ayub, 2003)

$Nu=0.2 Re^{0.75} Pr^{0.4}$, $10 < Re < 720$, water/glycol $(70 < Pr < 450)$ (27)

$Nu=0.248 Re^{0.75} Pr^{0.4}$ $1450 < Re < 11460$, water $(2.5 < Pr < 5.0)$....(28)

$f =12.065 Re^{-0.74}$ $10 < Re < 80$, water/glycol   (29)

$f =0.3323 Re^{-0.042}$ $1450 < Re < 11460$, water....(30)

$\beta = 30°$, $\varphi = 1.22$, A=0.32 m²,

$d_e =4.65$ mm

$L_p =0.946$ m, $\lambda=3.61$ mm, t =0.61 mm,

w =0.346 m

8.1.3 Coulson and Richardson

A correlation has been presented for turbulent single phase flow at Coulson and Richardson's book in which heat transfer coefficient and friction factor is gained as below: (Sinnott, 2005)

$$\frac{h.d_e}{k} = 0.26Re^{0.65}Pr^{0.4}(\frac{\mu}{\mu_w})^{0.14} \quad (31)$$

$$f = 0.6Re^{-0.3} \quad (32)$$

8.2   Flow boiling inside the evaporator

There are two types of boiling for a saturated liquid, flow boiling and pool boiling. In pool boiling the fluid is stationary but in flow boiling heat is transferred to a moving fluid. In a plate heat exchanger as an evaporator the fluid is moving, so flow boiling happens. In flow boiling also two different mechanisms are defined, convective evaporation and nucleate boiling. Convective evaporation is like the regular convective heat transfer in which the main resistance to heat transfer is at the heated wall of heat exchanger. In this mechanism, heat transfer correlations like to single phase heat transfer is used. In nucleate boiling, bubbles which form on the surface, transfer heat to the bulk of fluid. This mechanism is similar to pool boiling and is often modeled as pool boiling. For calculating total heat transfer both of these mechanisms are considered. A correction factor is applied for the pure nucleate and convective parts. The convective part is enhanced and developed by motions of the bubbles and in the other way the nucleate part; nucleation of bubbles is held back by flow of the liquid. The combined effects of these mechanisms are not recognized well. (Palm, 2007)

8.2.1   Ayub (2003)

For flow boiling Ayub has developed a correlation by 2003 in which the effect of chevron angle of plates are taken into account. It has the statistical error of 8%. All the values are in US units. C= 0.0675 for DX and C= 0.1121 for flooded and thermosiphons. (Ayub, 2003)

$$h_{tp} = C\left(\frac{k_L}{d_e}\right)\left(Re_L^2 \cdot \frac{h_{fg}}{L}\right)^{0.4124}\left(\frac{P}{P_{cr}}\right)^{0.12}\left(\frac{65}{\beta}\right)^{0.35} \quad (33)$$

$$f = \left(\frac{n}{Re^m}\right)(-1.89 + 6.56R - 3.69R^2) \ , 30 \ \leq \beta \leq 65 \quad (34)$$

Where,

$$R = \frac{\beta}{30}$$

$$\begin{cases} m = 0.137 \ , \ n = 2.99 & Re \ \leq 4,000 \\ m = 0.172 \ , n = 2.99 & 4,000 \ < \ Re \ \leq 8,000 \\ m = 0.161 \ , n = 3.15 & 8,000 \ < \ Re \ \leq 16,000 \\ m = 0.195 \ , n = 2.99 & 16,000 \ < \ Re \end{cases}$$

$$\Delta p = f\left(\frac{\rho w^2}{2}\right) \cdot \frac{L}{d} \quad (35)$$

In which h_{tp} is two phase heat transfer coefficient, β is chevron angle, P_{cr} is critical pressure, k_L is liquid thermal conductivity, L is plate length, f is friction factor. It is worth to mention that the calculated h_{tp} is in (Btu/hr.ft^2.°F) unit that can be converted to SI unit.

8.2.2   Cooper pool boiling correlation

Cooper in 1984 presented a new correlation including the surface roughness of the boiling surface.

$$h = 55 \cdot pr^{0.12-0.2logRp} (-log \ pr)^{-0.55} M^{-0.5} q^{0.67} \quad (36)$$

In case the surface roughness is unknown it has been suggested to set it equal to 1 μm.

Longo and Gasparella has shown in a study that heat transfer in flow boiling indicates great sensitivity to heat flux and nucleate boiling is the dominant mechanism which controls the vaporization. They also mentioned that Cooper correlation is a suitable equation to predict the heat transfer coefficient inside a small plate heat exchanger. (Longo et al., 2007)

Thus at this experiment in which heat flux in the evaporator is changing, Cooper pool boiling correlation has been applied.

8.3 Heat transfer calculation of the refrigerant

The total heat transfer in a plate heat exchanger can be calculated by this equation:

$Q = UA\Delta T_{LMTD}$ (37)

In which U is overall heat transfer coefficient, A is the heat transfer area and ΔT_{LMTD} is logarithmic mean temperature difference for pure counter current single phase heat exchanger which is defined as below,

$\Delta T_{LMTD} = \dfrac{\Delta T_1' - \Delta T_2'}{Ln\left(\frac{\Delta T_1'}{\Delta T_2'}\right)}$ (38)

The temperature profile for a counter current flow heat exchanger is like figure 14.
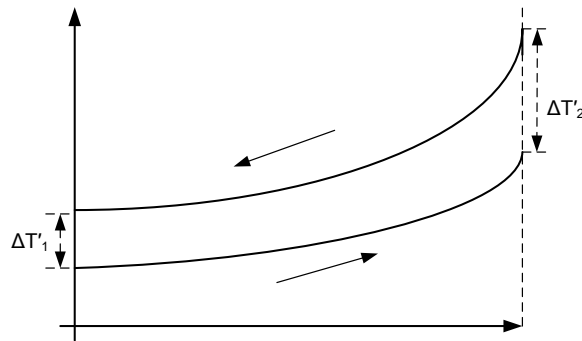
Figure 14.Schematic temperature profile in a heat exchanger with counter current flow.

Figure 15 shows idealized temperature profiles for single component fluids in a heat exchanger at different conditions.
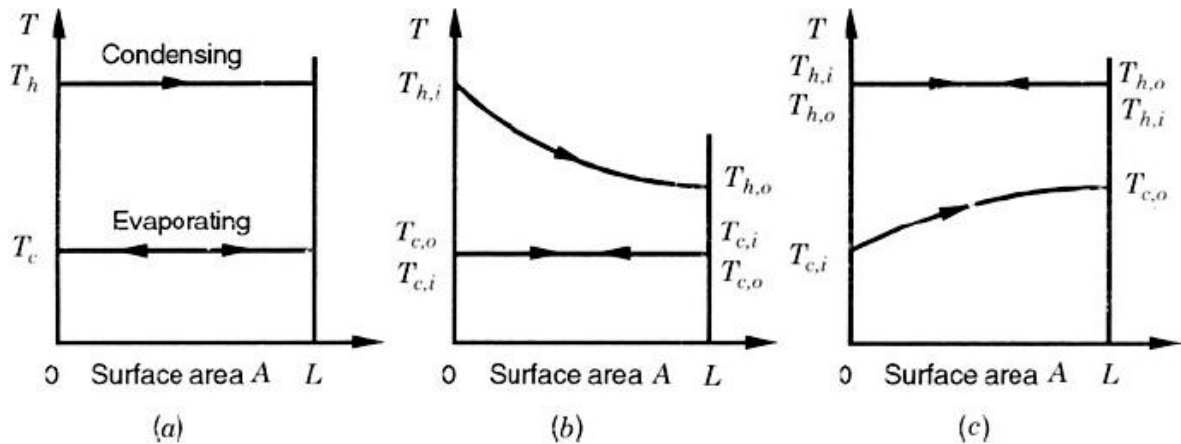
Figure 15.Idealized temperature profiles in case one or both fluids experience phase change

Fluids: (a) one of the fluids is condensing, and the other one is evaporating; (b) one single-phase fluid is cooling, the other one is evaporating; (c) one of the fluids is condensing, the other fluid is heating. (Shah, 2003)

For doing heat transfer analysis in a heat exchanger two basic equations are used: enthalpy rate equations and transferred heat through a secondary refrigerant. Enthalpy rate equation of refrigeration side and transferred heat from the secondary refrigerant of the heat exchanger are equal to the overall heat transfer:

$Q = m_r(h_{out} - h_{in}) = \left(mc_p\Delta T\right)_{secondray,r} = UA\Delta T_{LMTD}$ (39)

In which ΔT is equal to temperature change of secondary refrigerant from heat exchanger entrance to exit. The amount of heat which is conducted through the wall of heat exchanger is also equal to enthalpy rate change of the refrigerant side.

$$Q = A_r h_r (T_f - T_w) \quad (40)$$

h_r (W/m²K) represents convection heat transfer coefficient for refrigerant and A_r (m²). stands for plate surface area at refrigerant side. T_w (°C) indicates heat exchanger's wall temperature and T_f (°C) is the working fluid temperature. Finally with assumption of no fouling resistance the average heat transfer coefficient on the refrigerant side, h_r, is:

$$\frac{1}{A_r h_r} = \frac{1}{AU} - \frac{\Delta x}{A_2 k_w} - \frac{1}{A_1 h_{secondary\_r}} \quad (41)$$

k_w is thermal conductivity of the wall (W/mK), Δx is the wall thickness (m), A_2 is conductive heat transfer area through the wall, A_1(m²) shows heat transfer area in secondary refrigerant side, and A (m²) is overall heat transfer surface area. Since the amount of thermal resistance in the wall is much smaller than the fluid sides of heat exchanger it can be neglected. Overall heat transfer coefficient, U, can be evaluated through experimental values.

8.3.1 Heat transfer coefficient calculation by means of Wilson plot method

As equation 41 illustrates the wall temperature inside the heat exchanger is required in order to calculate convective heat transfer coefficient of refrigerant. However, when it is difficult to measure the wall temperature other methods like Wilson plot method are used. The Wilson plot method is applied to estimate the convective heat transfer coefficient, h, while both heat transfer coefficient of refrigerant and secondary refrigerant are unknown. Figure 16 illustrate a Wilson plot. Convective heat transfer coefficient in single phase flow can be expressed by the non-dimensional equation:

$$Nu = \frac{hd}{k} = C. Re^n Pr^m \quad (42)$$

In which,

$$Re = \frac{ud}{v} \quad (43) \text{ and } Pr = \frac{\mu C_P}{k} \quad (44)$$

Assuming that properties of the fluid don't change and convective heat transfer coefficient is a function of Re number.

$$h = C. Re^n \dots (45)$$

If the overall heat transfer coefficient U is referred to A_r and it is taken to account that at a plate heat exchanger, heat transfer area for refrigerant side (A_r) and secondary refrigerant side (A_1) are the same then from equation 39 and 41 can be concluded that,

$$\frac{1}{U} = \frac{1}{h_r} + \frac{A_1}{A_2} \times \frac{\Delta x}{k_w} + \frac{1}{h_{secondary\_r}} \quad (46)$$

So taking account equation 45 and 46 , overall heat transfer coefficient is obtained as a linear function of $1/Re^n$, in which the term of $1/h_{secondary\text{-}r}$ is the intercept of the line and over all heat transfer resistance axis and is constant. Therefore the equation 46 can be rearranged as below:

$$\frac{1}{U} = \frac{1}{CRe^n} + \text{constant} \quad (47)$$

When the $\frac{1}{U}$ is plotted versus $\frac{1}{CRe^n}$, all the points should make a straight line, if the exponent n is selected correctly.

As it is shown in figure 15 from the slope of the line the constant C can be calculated and so the value of h_r for each point can be obtained.

$$\frac{const}{h_r} = \frac{1}{\mathrm{Re}^n}$$
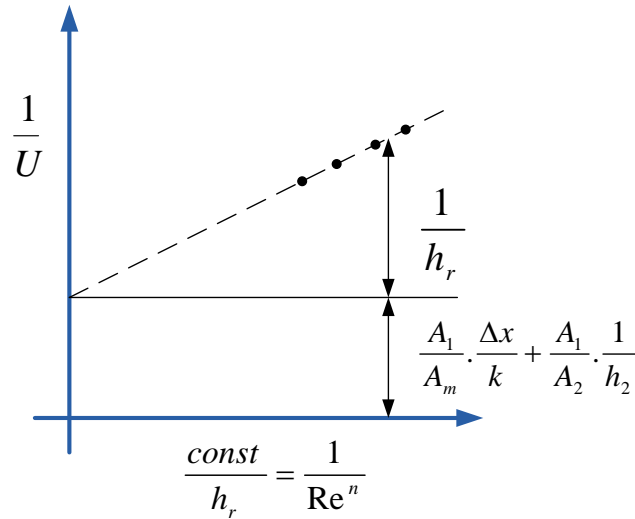
Figure 16.Wilson plot

Here it should be mentioned that the method assumes that the heat transfer coefficient on one side is not changed by changing flow rate on the other side. For boiling refrigerants this is not exactly true. The method should be used with care and awareness for evaporators. In this experiment the heat flux changes so it seems heat transfer coefficient of the refrigerant according to Cooper pool boiling correlation is mostly dependent on the heat flux. So equation 45 can be changed to:

h= C. q^n (48)

In figure 17 and 18 the mean value of experimental heat transfer coefficients of both R1234yf and R134a have been calculated by a modified Wilson plot method.
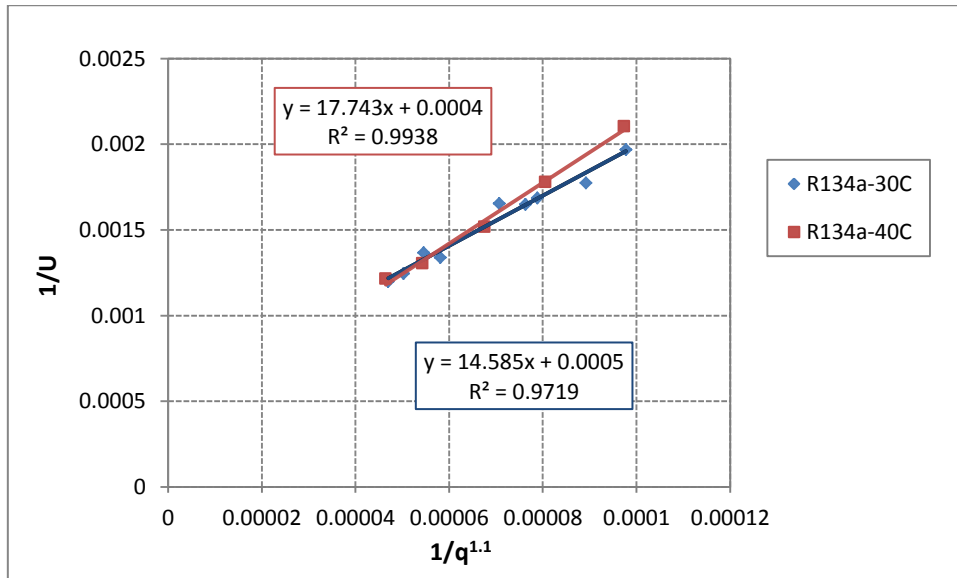
Figure 17.The modified Wilson plot for R134a at condensing temperatures of 30ºC and 40ºC for evaporator.

Figure 18.The modified Wilson plot for R1234yf at condensing temperatures of 30°C and 40°C for evaporator.

If Cooper-type correlation is applied, n=1.1 for heat flux exponent gives a straight line in the Wilson plot graph. So equation 48 can be expressed as $h_r = C \cdot q^{1.1}$ for this experiment. Intercept of $1/U$ vs $1/q^{1.1}$ plot is the heat transfer coefficient of the secondary refrigerant (brine) as well. In other words, equation 47 can be expressed as

$$\frac{1}{U} = \frac{1}{Cq^n} + \frac{1}{h_{brine}} \quad (49)$$

In which $\frac{1}{h_{brine}}$ is constant and is the intercept of the plotted line in Wilson plot graph. C is the slope of the line as well. Namely at condensing temperature of 30°C the coefficient C for R1234yf and R134a are 0.061 and 0.068 respectively and also at condensing temperature of 40°C the coefficient C is 0.043 for R1234yf and 0.056 for R134a. Consequently, heat transfer coefficients of refrigerants can be calculated by means of figure 17 and 18. (See the results in tables 5 to 8 of the appendix A.)

8.3.2 Heat transfer coefficient calculation by means of correlations

In section 8.3.1 heat transfer coefficient of the refrigerant has been gained by means of Wilson plot method. However, it is also possible to apply a suitable correlation from the literature in order to calculate heat transfer coefficient of the secondary refrigerant (brine). (See the brine properties in the appendix D.)

In this part Talik et al. correlation has been used to calculate the heat transfer coefficient of the brine. Heat exchanger characteristic mentioned for Talik et al. correlation is close to the exiting heat exchanger geometry in the test rig. Reynolds numbers for the water solution are 43-134, thus equation 27 has been used.

Consequently over all heat transfer coefficient from measured data and heat transfer coefficient of the brine from equation 27 can be applied in equation 46 in order to find heat transfer coefficient of the refrigerant. (See the results in tables 9 and 12 of the appendix A).

9 Results and discussion

9.1 Heat transfer in the evaporator

Experimental results were obtained at ten different heat loads of the electrical heater of the brine circuit. The condenser temperature was set for the first series of the tests, at 30℃ for both R134a and R1234yf, and for the second series of the tests, for both refrigerants was 40℃.Then in these conditions cycle performance, heat transfer at the evaporator and compressor performance have been investigated.

By means of equation 33 and experimental result, overall heat transfer coefficients of two refrigerants have been calculated. Comparing the overall heat transfer coefficients in the evaporator for both refrigerants, R134a has better and higher heat transfer performance than the new refrigerant. However, at higher refrigeration capacity it seems their overall heat transfer coefficients are getting the same and U ratio approaches to one. Analyzing the data also indicate at lower condenser temperature overall heat transfer coefficient is higher and the U of both refrigerants are closer to each other. Both figures 19 and 20 show the changes of U with increasing the cooling capacity for R1234yf and R134a. At higher heat loads, overall heat transfer coefficients of the two refrigerants are approaching each other so that at the last point, R1234yf has higher heat transfer coefficients.
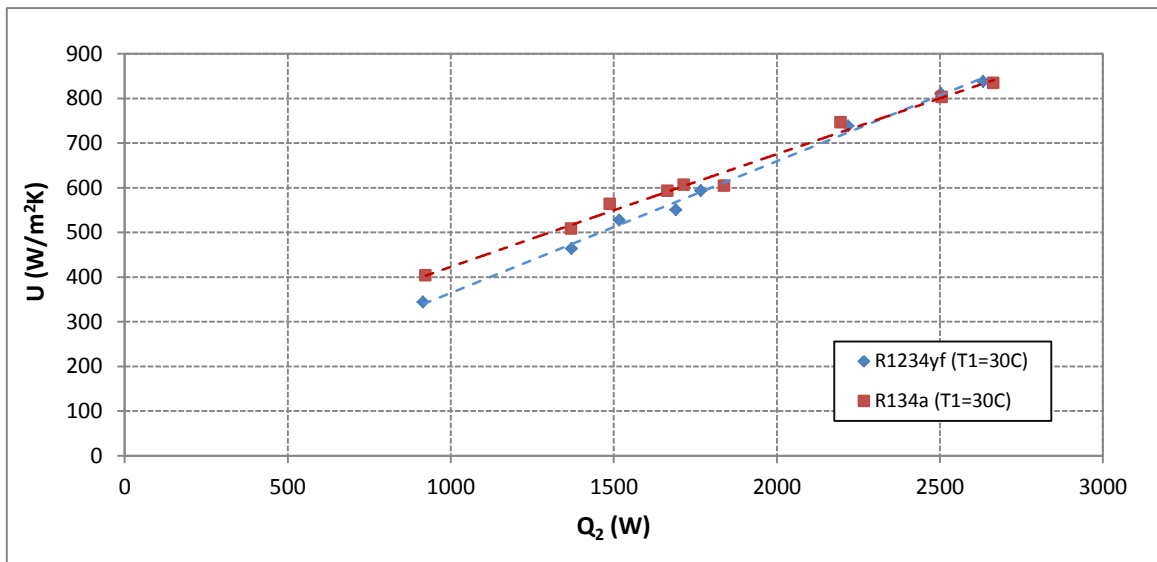
Figure19. Overall heat transfer coefficient in evaporator versus cooling capacity at condenser temperature 30℃.
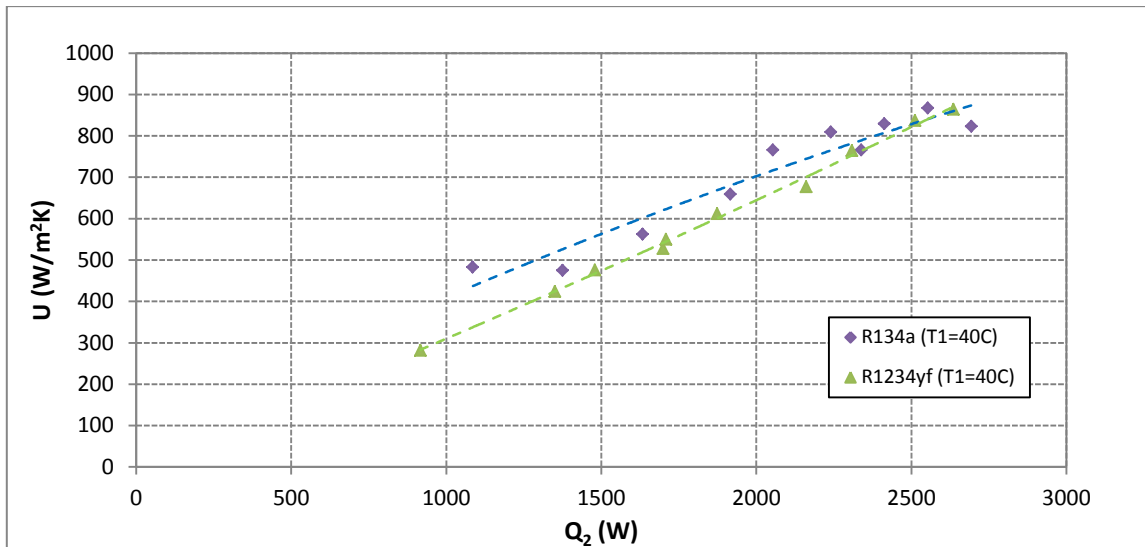
Figure 20 .Overall heat transfer coefficient in evaporator versus cooling capacity at condenser temperature 40ºC

Figure 20 also shows at higher heat loads the overall heat transfer coefficient values for both refrigerants are getting closer and even at the highest heat load the overall heat transfer coefficient of R1234yf is higher than R134a.

9.1.1 Using modified Wilson plot method for calculation of heat transfer coefficient

Similarly, as figure 21 and 22 indicate, heat transfer coefficients of two refrigerants are approaching by increasing the heat load.
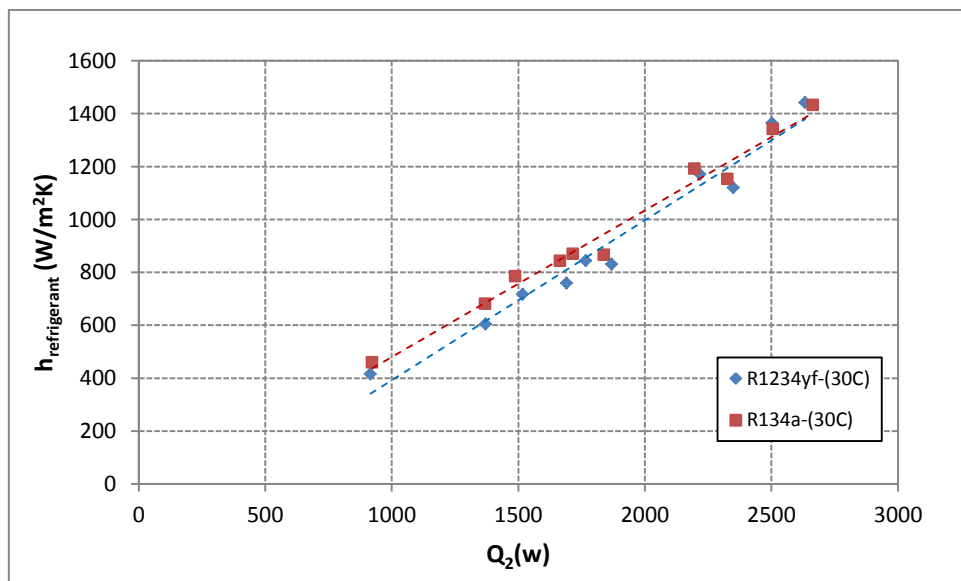
Figure 21. Heat transfer versus cooling capacity at condenser temperature 30ºC

From figure 21 and 22 the common refrigerant, R134a, obviously has better heat transfer characteristics than the new one, R1234yf at both condenser temperature of 30ºC and 40ºC. Heat transfer coefficients of R134a are higher than R1234yf by 4-12% and 9-36% at condensing temperature of 30ºC and 40ºC respectively.
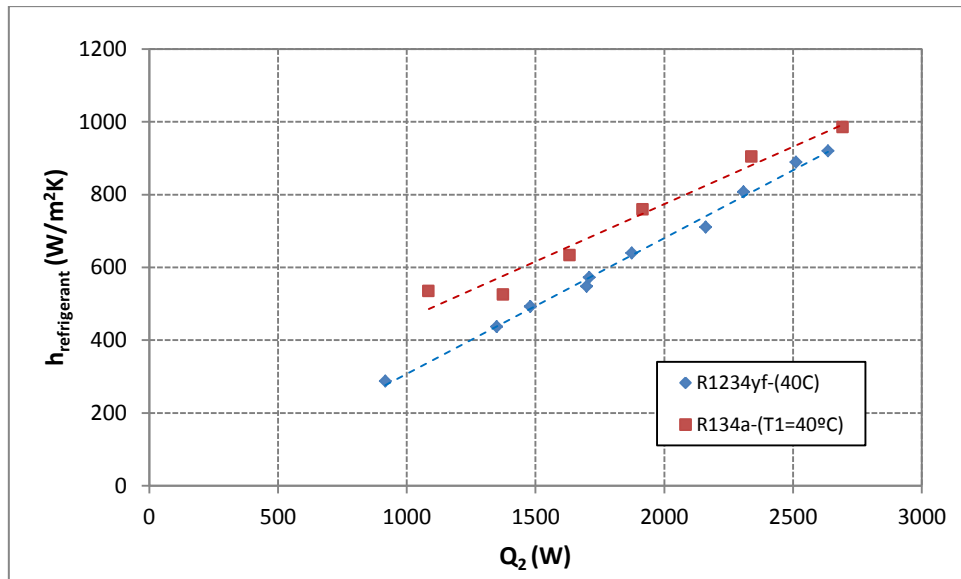
Figure22. Heat transfer versus cooling capacity at condenser temperature 40ºC

Heat transfer coefficient of the two refrigerants can be also calculated from the theoretical correlations. Since the geometrical characteristics of the plate are unknown Cooper correlation has been used here. For calculation of heat transfer coefficient, heat exchanger data sheet has been applied. See appendixes.

According to Cooper correlation, heat transfer coefficient of R1234yf is slightly higher than R134a by 2-5% while in the experiment, heat transfer coefficients of R1234yf are less than R134a by 4-12% and 9-38% at condensing temperature of 30ºC and 40ºC respectively. All the experimental results were plotted against the predicted values by Cooper correlations. The results were as indicated in figure 23

As figure 23 illustrates Cooper correlation overestimates the heat transfer coefficient. This is even more severe for R1234yf. Experimental data and theoretical values are even far from each other for the new refrigerant comparing to those for R134a. From figure 23, the heat transfer coefficients calculated by means of measured data agree with Cooper correlation within a range of -24-39% and -22-33% respectively for R1234yf and R134a. For example at q= 4420 (W/m²) and T_2= -4ºC, heat transfer coefficient of R1234yf from measured data is 604 (W/m²K) while at the same evaporating heat flux and temperature, heat transfer coefficient from Cooper correlation is 1006(W/m²K) which is 38% higher than measured value. At q= 4420 (W/m²), and T_2= -4ºC heat transfer coefficient of R134a from measured data is 681 (W/m²K) while at the same condition heat transfer coefficient form Cooper correlation is 973 (W/m²K) which is 29% higher that measured value.
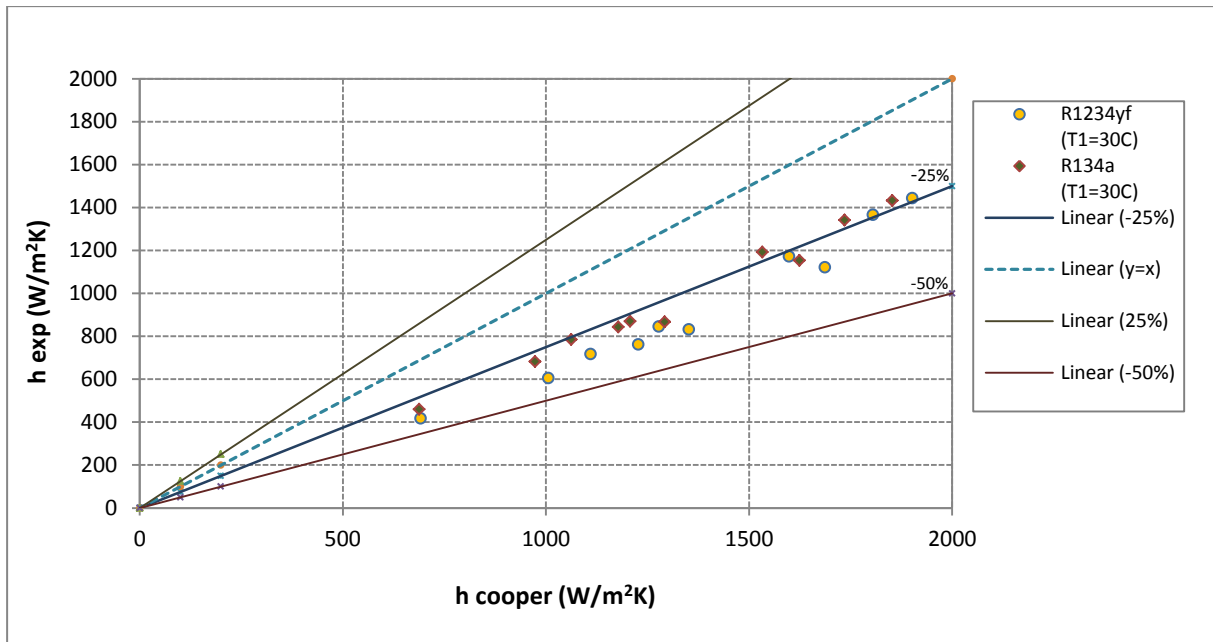
Figure 23 .Experimental heat transfer coefficient in the evaporator vs Predicted by Cooper pool boiling correlation for R1234yf and R134a.

9.1.2 Using Talik et al. correlation for calculation of Heat transfer coefficient

According to section 8.3.2, heat transfer coefficient of the refrigerant inside the evaporator can be estimated by means of correlations as well. In order to calculate heat transfer coefficient of the brine, Talik et al. correlation has been used. Figure 24 and 25 illustrate how heat transfer coefficient of the both refrigerants change with cooling capacity at two condensing temperature of 30ºC and 40ºC.
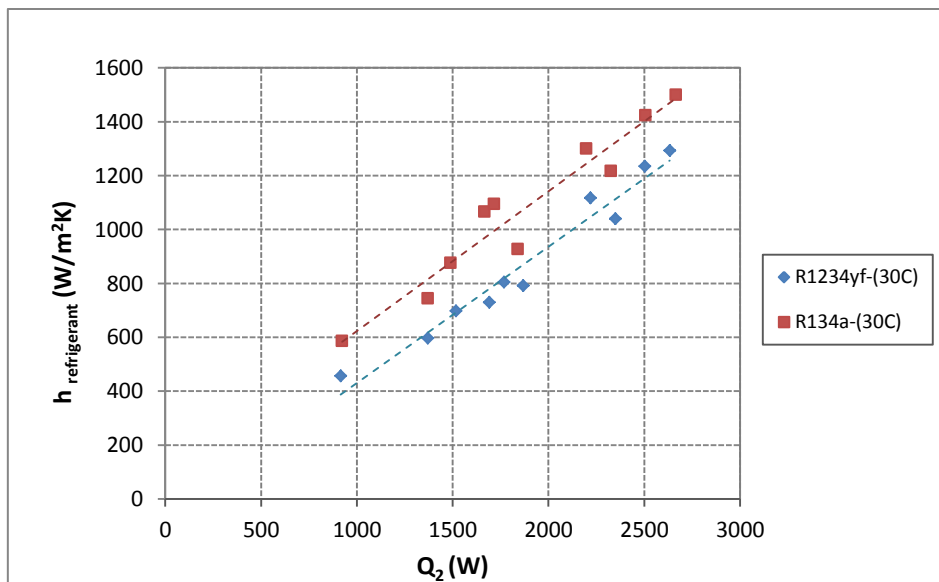
Figure 24 .Heat transfer versus cooling capacity at condenser temperature 30ºC

As figure 24 indicates, R134a has 13-22% higher heat transfer coefficients than those of R1234yf. Similarly, for condensing temperature of 40ºC, R134a has 8-39 % higher heat transfer coefficient than those for R1234yf. (Figure 25)
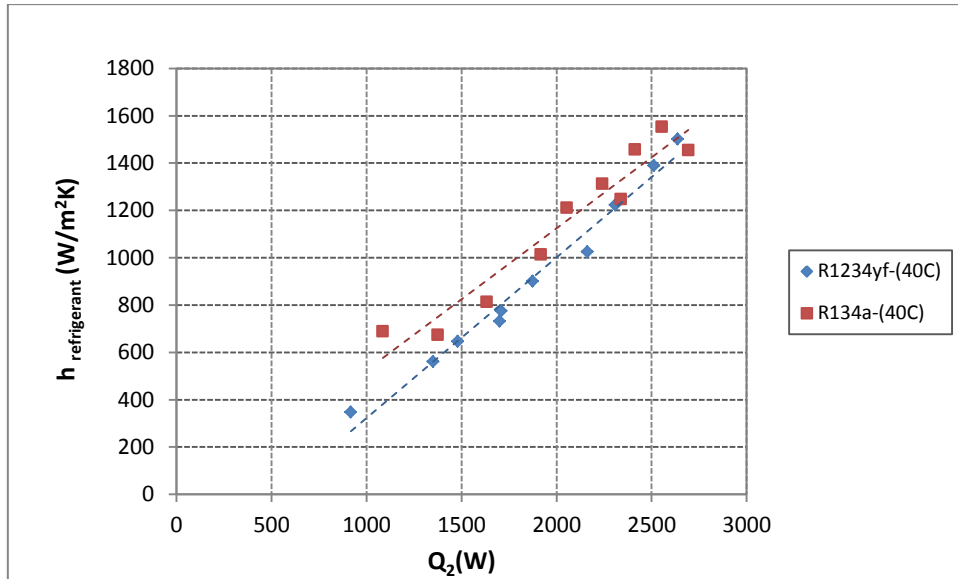
Figure 25 .Heat transfer versus cooling capacity at condenser temperature 40°C

Cooper correlation has been applied to calculate the heat transfer coefficient of both refrigerants at the same test condition. As the figure 26 explains Cooper correlation overestimates the heat transfer coefficient. This overestimation is even more for R1234yf. From figure 26, the heat transfer coefficients calculated by means of measured data agree with Cooper correlation within a range of -31 -41% and -9- 25% respectively for R1234yf and R134a.
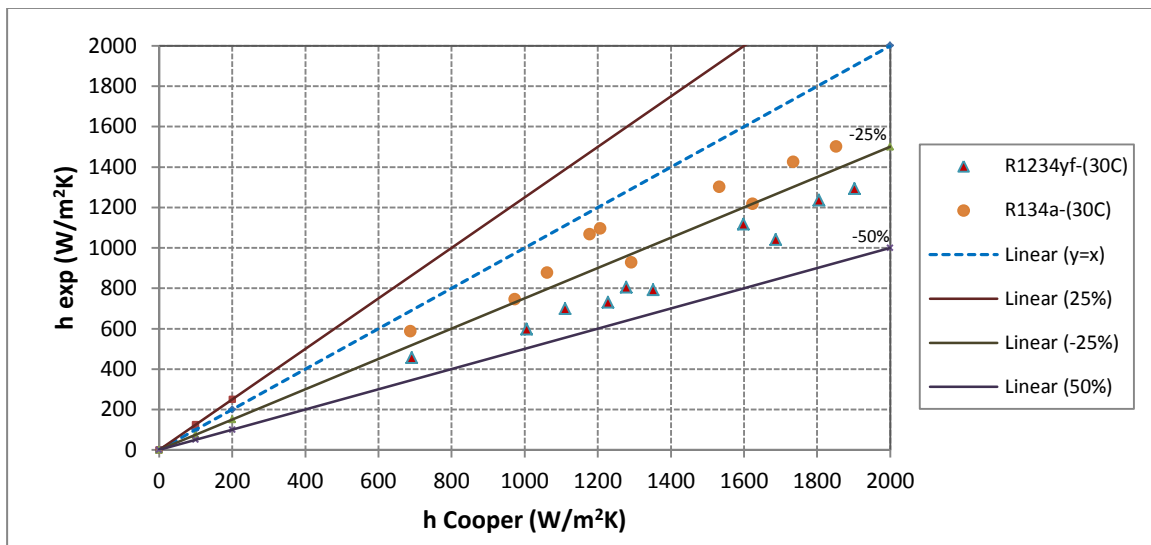
Figure 26 .Experimental heat transfer coefficient in the evaporator vs Predicted by Cooper pool boiling correlation for R1234yf and R134a

9.2   Heat transfer during condensation

For the condenser, Longo and Gasparella suggested a correlation for vertical plate heat exchanger using R-134a. (Longo et al., 2006)

$$h_r = \Phi 0{,}943[(k_l^3 \rho_l^2 g \Delta h_{fg})/(\mu_l \Delta TL)]^{0,25}   (46)$$

In which Φ is the enlargement factor (actual area/projected area), ΔT is temperature difference and L is plate length. Equation 42 has been applied to find the ratio of heat transfer coefficient of two refrigerants,

R1234yf and R134a. From the presented result in table 25, it can be predicted that HFO-1234yf has about 22% lower heat transfer coefficient than R-134a at both condensing temperature of 30ºC and 40ºC.

Table 25.Calculated ratio of condensation heat transfer coefficients of HFO-1234yf to R-134a

Condensing temperature (°C)	h_{R134a} (kW/m²K)	$h_{R1234yf}$ (kW/m²K)	h_{ratio}
30	317.05	247.70	0.78
40	291.56	227.66	0.78

Overall heat transfer coefficients are calculated from experimental data by means of equation 33. Overall heat transfer coefficients of R134a are higher than those of R1234yf at both condensing temperatures of 30ºC and 40ºC. Table 26 and 27 show U values of R1234yf calculated are approximately 22-33% lower rather than that of R134a at different condensing capacities.

Table 26.Experimental results at 30ºC at condenser.

Condensing capacity (kW)	U R134a (kW/m²K)	U R1234yf (kW/m²K)	U ratio
1.7	0.550	0.431	0.78
2.8	0.879	0.625	0.71
2.9	0.867	0.635	0.73

Table 27.Experimental results at 40ºC at condenser.

Condensing capacity (kW)	U R134a (kW/m²K)	U R1234yf (kW/m²K)	U ratio
2.6	0.748	0.497	0.67
2.8	0.714	0.539	0.75
2.9	0.760	0.599	0.78

9.3   Volumetric behavior

Thermodynamic properties of refrigerants help to calculate volumetric traits of them in refrigeration cycles. From figure 27 is found that volumetric refrigeration properties changes with evaporating temperature noticeably. Volumetric refrigeration effect of both refrigerants is increased by raising evaporating temperature and it is observed that refrigeration system has higher performance at higher evaporating temperatures and lower condensing temperature. Comparing the values at condensing temperature of 30°C, it is seen that at most of the points, the values are pretty close and even matching. At condensing temperature of 40°C by decreasing the evaporating temperature R-134a designates slightly higher refrigeration effect so that at the lowest point, R134a has 10% larger amount. Consequently, while in some points they have identical values, R134a operates averagely with 3% higher volumetric refrigerating effects.
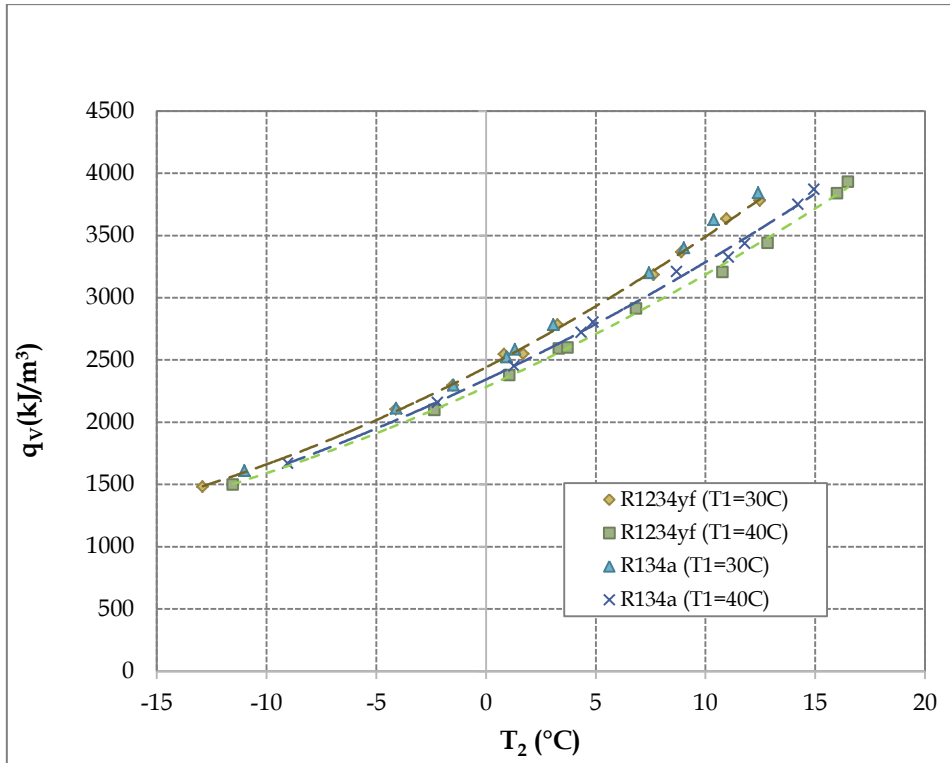
Figure 27.Volumetric cooling capacity of R1234yf and R134a for two condensing temperatures of 30°C and 40°C.

Figure 28 illustrates that the refrigeration systems require smaller compression work at lower condensing temperatures. Furthermore, R1234yf needs just about 0-7 % less volumetric compression work to run a refrigeration system with equal volume flow rate of vapor into the compressor at condensing temperature of 30°C. Similarly, at condensing temperature of 40C, R134a has about 0-8% higher volumetric compression work.
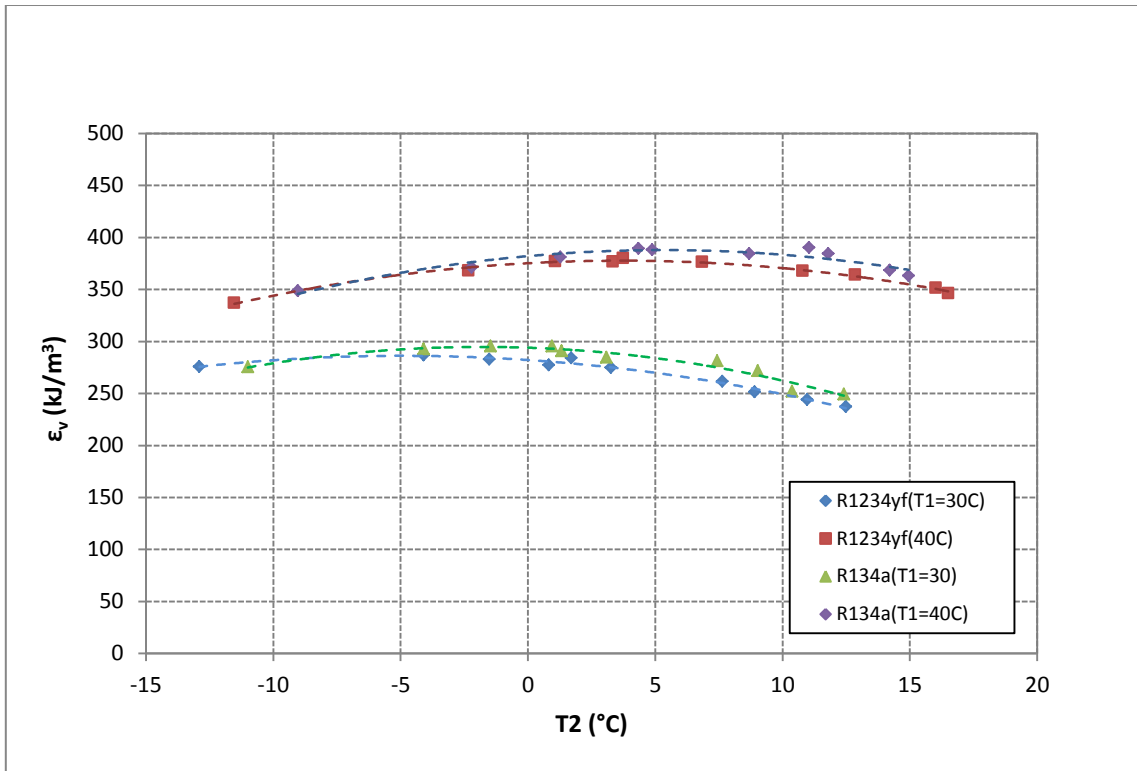
Figure 28.Volumetric compression work of R1234yf and R134a for two condensing temperatures of 30°C and 40°C.

9.4 Total isentropic efficiency

Total isentropic efficiency is defined as the ratio of the isentropic required work, ε_d, to the actual shaft work, ε_k. From figure 29, at condensing temperature of 30ºC, R1234yf has lower total isentropic compression efficiency than R134a.
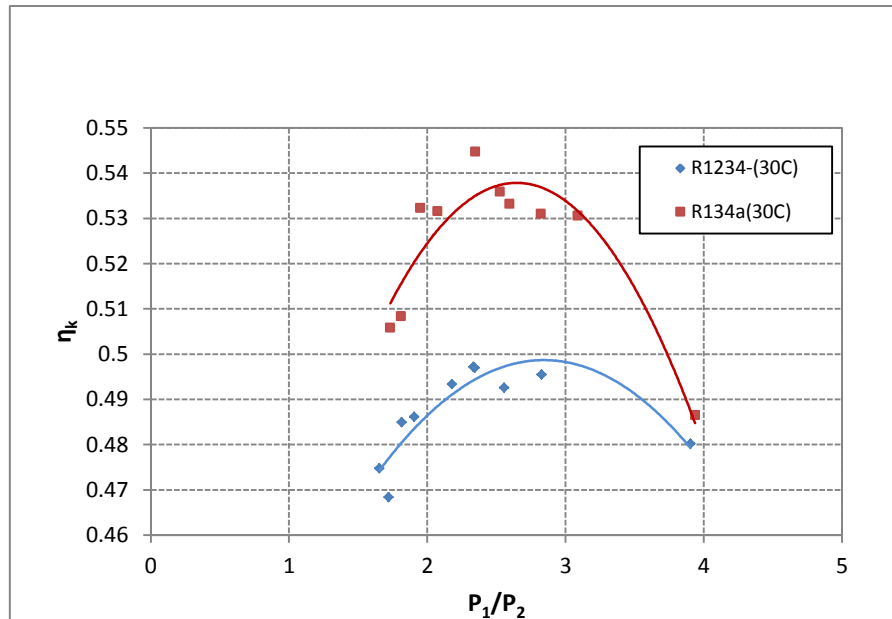
Figure 29. Total isentropic efficiency of R1234yf and R134a for condensing temperature of 30ºC.

The results for condensing temperature of 40ºC also show the same conclusion; isentropic compression efficiency of R134a is higher than R1234yf at each point.

9.5 Cycle performance

Coefficients of performances for both refrigerants have been calculated from the enthalpy differences at different heat loads for this experiment. Figure 30 shows COP_{2k} versus evaporating temperature. At condensing temperatures of 30ºC and 40ºC, R134a has respectively 2-10% and 5-15% higher COP_{2k} than the new refrigerant. For instance, at cooling capacity of 2kW, R134a has 3% and 14 % higher COP_{2k} than R1234yf respectively at condensing temperatures of 30ºC and 40ºC.
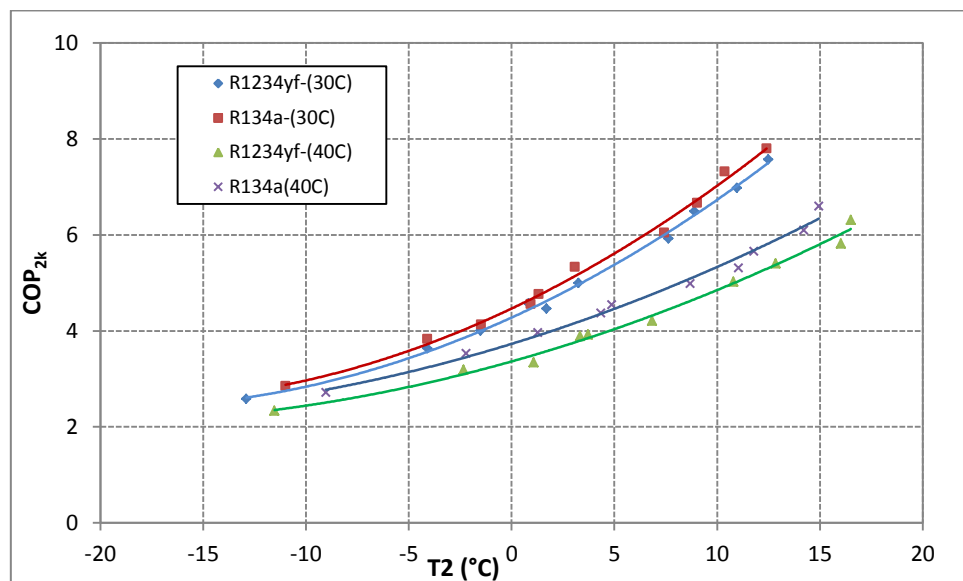
Figure 30. Cycle performance of R1234yf and R134a at two condensing temperatures of 30ºC and 40ºC.

10 Conclusion

High global warming potential of HFCs refrigerants have caused many environmental concerns. Therefore, many worldwide studies are being done in order to develop new alternatives which can mitigate the harmful ecological impacts of exiting refrigerants. There is an increasing interest to apply new candidates which can meet Kyoto Protocol suggestions. These materials should preferably be compatible with present equipment and technology and be commercialized soon. Refrigerants like carbon dioxide, ammonia, hydrocarbons, R152a, HFO-1234yf and HFO-1234ze have low GWP and acceptable potential to replace the common refrigerants. Flammability is the matter of discussion on these alternatives. Although both R1234yf and R1234ze have been considered as candidates for substituting common refrigerants and the performed experiments indicate promising performances of these two new refrigerants, it is required to do more experiments in different type of cycles and conditions in order to utilize these refrigerants.

In this study, theoretical cycle data indicates R1234ze has about 3% higher pressure ratio than R134a while R1234yf has 9% lower pressure ratio than R134a. Furthermore, both new refrigerants have approximately the same discharge temperatures; however, they have lower values than those of R134a. It can be concluded from the cycle data tables that COP_{2d} of R1234ze is about 1% lower than R134a and it is about 3% higher than R1234yf as well.

From drop-in test of R1234yf and R134a can be drawn that R134a has averagely 0-3% higher volumetric cooling capacity and 0-8% higher volumetric compression work than those for R1234yf respectively at both condensing temperature of 30ºC and 40ºC. Coefficient of performance of R1234yf is 2-9.2% lower than that of R134a at condensing temperature of 30ºC and 4.4-15% lower at 40ºC.

In term of heat transfer, experimental flow boiling heat transfer of both R1234yf and R134a have been investigated. The average heat transfer coefficients in plate heat exchanger evaporators were evaluated at heat loads of 1-3.2 kW and two condensing temperatures of 30ºC and 40ºC. Results show R134a has higher heat transfer coefficients than R1234yf. However, differences between heat transfer coefficients are higher at lower heat loads and by increasing the heat loads the difference decreases slightly. For calculating the heat transfer coefficient of the refrigerants two methods have been applied. At first approach, by means of modified Wilson method, heat transfer coefficients were calculated and at the second method, heat transfer coefficient of the brine was evaluated by a suitable correlation and subsequently heat transfer coefficient of the refrigerants computed. Calculated experimental heat transfer by means of modified Wilson plot method indicates R134a has about 4-12% higher heat transfer coefficients than R1234yf at T_1=30ºC and also 9-36% higher heat transfer coefficients at T_1=40ºC. Moreover, the heat transfer coefficients gained by measured data agree with those predicted by Cooper correlation within ranges of -22-33% and -24-39% for R134a and R1234yf respectively. Using Talik et al. correlation to find heat transfer coefficient of the brine results in 22-32% higher heat transfer coefficient values comparing to those from modified Wilson plot method.

Bibliography

Akasaka R., 2010 "*An application of the extended corresponding states model to thermodynamic property calculations for trans-1,3,3,3-tetrafluoropropene (HFO-1234ze(E))*", International Journal of Refrigeration, 33(2010)907 e9 1 4 ,Elsevier Ltd and IIR, March 2010.
Available at < www. Scincedirect.com>

Akasaka R. , Tanaka K, Higashi Y., 2009, *Thermodynamic property modeling for 2,3,3,3-tetraflouropropene(HFO-1234yf)*, International Journal of Refrigeration, 33(2010)52-60 ,Elsevier Ltd and IIR, September 2009 ,Available at < www. Scincedirect.com>

Arcakliogˇlu E., Avusogˇlu A. C, Erisen A.," *Thermodynamic analysis of refrigerant mixtures for possible replacements for CFCs by an algorithm compiling property data*", Applied Thermal Engineering ,26 (2006) 430–439, Elsevier LTD, August 2005.

Available at < www. Scincedirect.com>

Ashrae Standard, 2010, *Designation and Safety Classification of Refrigerants*, American Society of Heating, Refrigerating and Air-Conditioning Engineers, Inc. ISSN 1041-2336.

Atkinson R., Baulch D. L., Cox R. A., Crowley J. N., Hampson R. F., Hynes R. G., Jenkin M. E., Rossi M. J., Troe J., and Wallington T. J., 2008, *Evaluated kinetic and photochemical data for atmospheric chemistry: Volume IV – gas phase reactions of organic halogen species,* Atmospheric Chemistry and Physics Journal, Atmos. Chem. Phys., 8, 4141–4496, 2008

Ayub, Z.H. 2003, *Plate Heat Exchanger Literature Survey and New Heat Transfer and Pressure Drop Correlations for Refrigerant Evaporators*, Heat transfers Engineering 24(5):3-16.

Benni Du, Changjun Feng, Weichao Zhang, 2009, *Theoretical studies on the reaction mechanisms and rate constants for OH radicals with CF3CF@CH2*, Chemical Physics Letters 479 (2009) 37–42, Elsevier B.V. Available at < www. Scincedirect.com>

Brown J.S., Zilio C., Cavallini A. *Thermodynamic properties of eight fluorinated olefins ,* International Journal of Refrigeration, 33(2010)235-241 ,Elsevier Ltd and IIR, May 2009.

Available at < www. Scincedirect.com>

Dossat, Roy J. 1991. *Principles of Refrigeration*, 3rd Edition, New Jersey, Prentice Hall, Inc., 1991. ISBN: 0-13-717687-2.

Davis, 2008, *Uniform Mechanical Code,* Chapter 11, Table 11-1 – Refrigerant Groups, Properties and Allowable Quantities, ASHRAE Standards.
Available at:
<http://www.iapmo.org/Tentative%20Interim%20Amendments/UMC%20Extracts/2008%20UMC%20Extracts%20Table%2011-1%20Issued.pdf >

Fact Sheet, 2011, Occupational health and safety, Honeywell Company.

Available at < http://www.1234facts.com/pdf/FactSheet_E_HSE_110307.pdf>

Fleischer R., 2010, *Latest Developments in Refrigerants, Combi Cool Winterdays* 17.-18.2.2010, Honeywell Fluorine Products, Available at: <http://www.combicool.fi/sivut/assets/files/Talvipaivat_2010/CC2010_Honeywell.pdf >

Granryd, Eric ,2005 *,Refrigerant Cycle Data,* Thermophysical properties of refrigerants for applications in vapor compression systems, Department of Energy Technology, KTH, Stockholm.

Granryd, Eric, et al. 2005. *Refrigeration Engineering,* 5th Edition, Stockholm: Royal Institute of Technology, KTH, 2005, Vol. I.

Hamdar M., Zoughaib A., Clodic D.,2010 ,"*Flow boiling heat transfer and pressure drop of pure HFC-152a in a horizontal mini-channel*", International Journal of Refrigeration, Volume 33, Issue 3,

Pages 566-577, Elsevier Ltd and IIR, May 2010.

Available at < www. Scincedirect.com>

Hill William, 2010, *Industry 3 year evaluation of low global warming potential refrigerant HFO-1234yf,* Dupont Company.

Availableat:

<http://www2.dupont.com/Refrigerants/en_US/assets/downloads/SmartAutoAC/20100121_MACS_ Hill_summary.pdf >

Hrnjak. P. S., Richter. M. R, Bullard. C. W., Comparison of R744and R410A for Residential Heating and Cooling Applications", ACRC ,CR-39, University of Illinois, June 2001.

Honeywell, *HFO-1234ze Blowing Agent," trans – 1,3,3,3-tetrafluoropropene*", Honeywell International Inc,2008,The Netherlands
Available at < http://www51.honeywell.com/sm/lgwp-uk/common/documents/FP_LGWP_UK_Honeywell-HFO-1234ze_Literature_document.pdf

Hughes J, Kontomaris K., Leck T.J., 2010, A Non-Flammable, Reduced GWP, HFC-134a Replacement in Centrifugal Chillers: DR-11, 1DuPont Fluorochemicals R&D, International Refrigeration and Air Conditioning Conference at Purdue
Available at < http://www2.dupont.com/Refrigerants/en_US/assets/downloads/20100612-IRAC-Kontomaris-Leck-Hughes-paper.pdf >

Jarall S., 2010*,"Properties of new GWP refrigerants*", ETT, Energiteknik,   KTH, Stockholm.

Jung D., "*Energy and environmental crisis: let's solve it naturally in refrigeration and air conditioning* ", American Society of Heating, Refrigerating, and Air-Conditioning Engineers, Inc. September 2008. Available at: <http://www.thefreelibrary.com/Energy+and+environmental+crisis%3A+let%27s+solve+it+naturally+ in...-a0186399834 >

Kajihara Hideo, Inoue Kazuya, Yoshida Kikuo, Ryuichi Nagaosa, 2010, *Estimation of environmental concentrations and deposition fluxes of R-1234-YF and its decomposition products emitted from air conditioning equipment*

to atmosphere, International Symposium on Next-generation Air Conditioning and Refrigeration Technology Conference, 17 – 19 February 2010, Tokyo, Japan. Saga University Japan.

Kilicarslan A., Hosoz M.,” *Energy and irreversibility analysis of a cascade refrigeration system for various refrigerant couples”, Energy conversion and management*, 51 (2010) 2947-2954, Elsevier LTD ,July 2010.

Available at <www. Scincedirect.com.>

Koban Mary, 2009, *HFO-1234yf Low GWP Refrigerant, LCCP Analysis*, SAE 2009 World Congress.

Available at
http://www2.dupont.com/Refrigerants/en_US/assets/downloads/SmartAutoAC/MAC_HFO_1234yf_SAE_04202009.pdf

Koban Mary, 2010, *HFO-1234yf Low GWP Refrigerant, Information for manufacturing and service facilities*, Dupont Company.

Available at:

<http://www2.dupont.com/Refrigerants/en_US/assets/downloads/SmartAutoAC/2010_AutomotiveSummit_HFO-1234yf_LowGWP.pdf>

Kontomaris K., Leck T.J., Hughes J., 2010, Low GWP refrigerants for air condoning of large buildings, Dupont Flurochemicals R&D. Available at :
http://www2.dupont.com/Refrigerants/en_US/assets/downloads/20100309-CLIMA-Kontomaris-Leck-Hughes-paper.pdf >

Korfitsen V, Kristensen A.P.R., “Ammonia high pressure heat pumps in food refrigeration applications” ,Elsevier Science Ltd and IIR,PII:S0140-7007(98)00012-7,January 1998.

Kontomaris K. (Kostas), 2010, A low GWP replacement for HCFC-123 in centrifugal chillers: DR-2, Dupont Company.
Available at :
http://www2.dupont.com/Refrigerants/en_US/assets/downloads/20101001_UNEP_Kontomaris_paper.pdf

Koyama S., Takada N., Matsuo Y., Yoshitake D., Fukuda S., ”Possibility to introduce HFO-1234ze(E) and its mixture with HFC-32 as low-GWP alternatives for heat pump/refrigeration systems”, Internationals Symposium on Next-generation Air Conditioning and Refrigeration Technology Conference, 17 - 19 February 2010, Tokyo, Japan

Lee H.S., Yoon J.I., Kim J.D., Bansal P.,” Evaporating heat transfer and pressure drop of hydrocarbon refrigerants in 9.52 and 12.70 mm smooth tube” , International Journal of Heat and Mass Transfer ,48 (2005) 2351–2359 , Elsevier LTD, Available at Science Direct ,March 2005.
Available at <www. Scincedirect.com.>

Leck T.J, 2009, Evaluation of HFO-1234yf as a potential replacement for R-134ain refrigeration applications, 3rd IIR Conference on thermophysical properties and transfer processes of refrigerants, Boulder, CO, US.

Lemmon, E.W., Huber, M.L., McLinden, M.O., 2010, NIST Standard Reference Database 23:, Reference Fluid Thermodynamic and Transport Properties-REFPROP, Version 9.0, National Institute of Standards and Technology, Standard Reference Data Program, Gaithersburg, 2010.

Longo G.A., Gasparella A., 2007, Heat transfer and pressure drop during HFC-134a condensation inside a brazed plate heat exchanger, in: International Congress of Refrigeration, Beijing, 2007.

Longo G.A., Gasparella A., 2006, Heat transfer and pressure drop during HFC refrigerant saturated vapor condensation inside a brazed plate heat exchanger, International journal of heat transfer 53(2010) 1079-1087, Elsevier Ltd. Available at <www. Scincedirect.com.>

Material Safety Data Sheet," HFO-1234ze, HBA-1", Version 1.6, Honeywell Fluorine Products Europe B.V Honeywell Fluorine Products Europe B.V., September 2008, The Netherlands.

Available at < http://www51.honeywell.com/sm/lgwp-uk/common/documents/msds-documents/FP_LGWP_UK_HFO-1234ze_uk_MSDS.pdf >

Mathur G.D., Heat transfer coefficient and pressure gradients for refrigerant R-152a, Alternate Refrigerant System Symposium, Phoenix, AZ, July 16, 2003

Available at:< http://www.sae.org/altrefrigerant/presentations/presw-mathur.pdf>

Matsuguchi A., Kagawa N., Koyama S., Study on Isochoric Specific Heat Capacity of Liquid OF-1234ze(E), International Symposium on Next-generation Air Conditioning and Refrigeration Technology Conference, 17 – 19 February 2010, Tokyo, Japan. National Defense Academy, Yokosuka, Japan

Melinder Å., 2010, *Properties of secondary working fluids for indirect systems*, International Institute of Refrigeration, IIR., Paris, France.

Miyara A., Tsubaki K., Sato N., Thermal conductivity of HFO-1234ze(E)+HFC-32 Mixture, International Symposium on Next-generation Air Conditioning and Refrigeration Technology Conference, 17 – 19 February 2010, Tokyo, Japan. Saga University Japan.

MSDS, Material Safety Data Sheet," HFO-1234yf (2,3,3,3-Tetrafluoro-1-propene)" , DuPont Chemical Solutions Enterprise, 05574925,September 2010, USA.

Available at < http://msds.dupont.com/msds/pdfs/EN/PEN_09004a2f806513e4.pdf

Nielsen O.J. , Javadi M.S., Sulbaek M.P., Andersen A., Hurley M.D., Wallington T.J. , Singh R. ,2007,*Atmospheric chemistry of CF3CF@CH2: Kinetics and mechanisms of gas-phase reactions with Cl atoms, OH radicals, and O3* ,Chemical Physics Letters 439 (2007) 18–22, Elsevier B.V.

Available at < www. Scincedirect.com>

Palm B., Claesson J., 2005, Plate *Heat Exchangers: Calculation Methods for Single and Two-Phase Flow, Heat Transfer Engineering*, 27(4):88-98,2006

Reimer Horst-Ulrich, 2010, *DuPont™ Opteon™ XP10: A new option for more environmentally sustainable commercial refrigeration*, DuPont Chemicals & Fluoroproducts.

Available at :< http://www2.dupont.com/Refrigerants/en_US/assets/downloads/article20101014.pdf >

Richter M., McLinden M.O., and Lemmon E.W., 2010,"Thermodynamic Properties of 2,3,3,3-Tetrafluoroprop-1-ene (R1234yf): p-rho-T, Measurements and an Equation of State," Journal of Chemical and Engineering Data, (to be submitted) 2010.

SAE International, 2009, Industry evaluation of low global warming potential refrigerant HFO-1234yf, SAE CRP1234.
Available at :< http://www.sae.org/standardsdev/tsb/cooperative/crp1234-3.pdf >

Samuel F. Yana Motta, Elizabet D. Vera Becerra, Mark W. Spatz, 2010, *Low global warming alternatives refrigerants for stationary AC&R applications*, Honeywell International, Buffalo Research Laboratory, International Refrigeration and Air Conditioning Conference at Purdue.

Sawalha S., 2009, *Using CO2 in Supermarket Refrigeration*, ASHRAE Journal, Vol.47, No.8, 26-30, Aug-2005.

Sinnott R.K, 2005, *Coulson and Richardson's Chemical Engineering* Volume 6 - Chemical Engineering Design (4th Edition), Elsevier, pp.759-763

Shah R. K., Sekulić Dušan P.,2003 ,*Fundamental of heat exchanger design*, John Wiley & Sons,pp.231-239

Schustera P., Bertermannb R., Ruschc G., Dekant W., 2009, Biotransformation of trans-1,1,1,3-tetrafluoropropene (HFO-1234ze), Toxicology and Applied Pharmacology, Volume 239, Issue 3, 15 September 2009, Pages 215–223.

Skander Jribia, Bidyut Baran Sahab, Shigeru Koyamaa, Anutosh Chakrabortyc, Kim Choon Ng, 2011, Study on activated carbon/HFO-1234ze(E) based adsorption cooling cycle, Applied Thermal Engineering, Elsevier LTD.

Available at < www. Scincedirect.com>

Tanaka K., Higashia Y., 2010 , Thermodynamic properties of HFO-1234yf (2,3,3,3-tetrafluoropropene) Propriétés thermodynamiques du HFO-1234yf (2,3,3,3-tétrafluoropropène) , Refrigeration, Volume, Pages 474-479.

Available at < www. Scincedirect.com>

Taria S., Nakai A., Piao. C., *Examination regarding Air Conditioning and Heat Pump Water Heater System using Post New alternative Refrigerant*, International Symposium on Next-generation Air Conditioning and Refrigeration Technology Conference, 17 – 19 February 2010, Tokyo, Japan .DAIKIN Industries. Ltd , 2010,Japan.

Toxicity Summery, 2010, *Significant Toxicity Information Available*, DuPont Chemical Solutions Enterprise
Available at:
<http://www2.dupont.com/Refrigerants/en_US/assets/downloads/SmartAutoAC/toxicity_summary.pdf>

Appendix A

Table 1.Results from experiment at condensing temperature = 30°C for R1234yf

Brine Heat load (kW)	P_{diff} (mbar)	m_r (gr/s)	P_2 (bar)	P_1 (bar)	T_2 (°C)	Refrigeration Capacity (kW)	Condenser heat load(kW)	Power to the shaft (kW)	η_s (volumetric efficiency)	COP_{Real}	UA $_{Evaporator}$ (kW/K)	UA $_{Condenser}$ (kW/K)
1.00	0.02	6.71	1.99	7.78	-12.91	0.92	1.27	0.35	0.85	2.58	0.11	0.22
1.50	0.04	9.56	2.75	7.76	-4.10	1.37	1.75	0.38	0.89	3.63	0.14	0.27
1.70	0.04	10.59	3.00	7.67	-1.51	1.52	1.90	0.38	0.91	4.00	0.16	0.32
2.00	0.04	12.31	3.35	7.81	1.70	1.77	2.16	0.40	0.95	4.46	0.18	0.33
2.15	0.04	12.48	3.53	7.68	3.26	1.87	2.24	0.37	0.92	5.00	0.18	0.34
2.00	0.04	11.43	3.25	7.61	0.82	1.69	2.06	0.37	0.91	4.56	0.17	0.33
2.50	0.05	14.91	4.06	7.74	7.64	2.22	2.59	0.37	0.96	5.92	0.23	0.39
2.70	0.04	15.43	4.23	7.67	8.90	2.35	2.71	0.36	0.96	6.49	0.22	0.38
3.00	0.04	16.29	4.51	7.76	10.97	2.50	2.86	0.36	0.94	6.98	0.25	0.39
3.20	0.04	17.20	4.73	7.82	12.49	2.63	2.98	0.35	0.96	7.57	0.26	0.39

Table 2.Results from experiment at condensing temperature = 40°C for R1234yf

Brine Heat load (kW)	P$_{diff}$ (mbar)	m$_r$ (gr/s)	P$_2$ (bar)	P$_1$ (bar)	T$_2$ (°C)	Refrigeration Capacity (kW)	Condenser heat load(kW)	Power to the shaft (kW)	η$_s$ (volumetric efficiency)	COP$_{Real}$	UA $_{Evaporator}$ (kW/K)	UA $_{Condenser}$ (kW/K)
1.00	0.01	6.93	2.10	10.26	-11.53	0.92	1.31	0.39	0.84	2.33	0.09	0.23
1.50	0.03	9.98	2.92	10.28	-2.34	1.35	1.77	0.42	0.88	3.19	0.13	0.27
1.70	0.03	10.79	3.28	10.37	1.07	1.48	1.92	0.44	0.85	3.34	0.15	0.28
2.00	0.04	12.20	3.53	10.30	3.34	1.70	2.14	0.44	0.90	3.89	0.16	0.29
2.15	0.03	13.41	3.96	10.30	6.85	1.87	2.32	0.45	0.88	4.21	0.19	0.30
2.00	0.04	12.40	3.58	10.39	3.73	1.71	2.14	0.44	0.90	3.92	0.17	0.28
2.50	0.03	15.79	4.49	10.25	10.79	2.16	2.59	0.43	0.93	5.02	0.21	0.38
2.70	0.05	16.79	4.78	10.30	12.85	2.31	2.74	0.43	0.92	5.40	0.24	0.31
3.00	0.06	17.99	5.26	10.32	16.02	2.51	2.94	0.43	0.90	5.81	0.26	0.33
3.20	0.06	18.69	5.34	10.28	16.51	2.64	3.05	0.42	0.92	6.31	0.27	0.37

Table 3.Results from experiment at condensing temperature = 30°C for R134a

Brine Heat load (kW)	P_{diff} (mbar)	m_r (gr/s)	P_2 (bar)	P_1 (bar)	T_2 (°C)	Refrigeration Capacity (kW)	Condenser heat load(kW)	Power to the shaft (kW)	η_s (volumetric efficiency)	COP_{Real}	$UA_{Evaporator}$ (kW/K)	$UA_{Condenser}$ (kW/K)
1.00	0.018	5.35	1.93	7.59	-11.00	0.92	1.27	0.325	0.786	2.91	0.128	0.426
1.50	0.024	7.75	2.52	7.78	-4.09	1.37	1.75	0.358	0.890	3.89	0.160	0.346
1.70	0.030	8.55	2.78	7.83	-1.47	1.49	1.90	0.361	0.890	4.26	0.180	0.345
2.00	0.028	9.43	3.03	7.86	0.94	1.67	2.07	0.366	0.906	4.66	0.188	0.361
2.15	0.036	10.07	3.27	7.68	3.08	1.84	2.18	0.345	0.906	5.33	0.188	0.378
2.00	0.032	9.60	3.07	7.76	1.32	1.72	2.10	0.360	0.910	4.84	0.191	0.370
2.50	0.036	12.22	3.80	7.88	7.43	2.20	2.56	0.364	0.942	6.04	0.232	0.394
2.70	0.044	12.72	4.01	7.83	9.03	2.33	2.68	0.349	0.938	6.66	0.227	0.390
3.00	0.040	13.48	4.20	7.60	10.38	2.51	2.81	0.343	0.948	7.20	0.245	0.538
3.20	0.047	14.35	4.49	7.78	12.41	2.66	3.01	0.342	0.952	7.79	0.259	0.538

Table 4.Results from experiment at condensing temperature = 40°C for R134a

Brine Heat load (kW)	P_{diff} (mbar)	m_r (gr/s)	P_2 (bar)	P_1 (bar)	T_2 (°C)	Refrigeration Capacity,q_v (kW)	Condenser heat load(kW)	Power to the shaft ε_k (kW)	η_s (volumetric efficiency)	COP_{Real}	$UA_{Evaporator}$ (kW/K)	$UA_{Condenser}$ (kW/K)
1.00	0.026	6.54	2.08	10.36	-9.04	1.09	1.40	0.400	0.893	2.50	0.138	-
1.50	0.030	8.14	2.70	10.23	-2.21	1.38	1.75	0.390	0.875	3.49	0.146	-
1.70	0.031	9.61	3.07	10.29	1.28	1.63	1.98	0.412	0.914	3.79	0.167	-
2.00	0.034	11.97	3.48	10.38	4.88	2.05	2.31	0.452	1.004	4.12	0.215	-
2.15	0.040	12.94	3.97	10.30	8.70	2.24	2.50	0.450	0.958	4.56	0.230	-
2.00	0.037	11.31	3.42	10.42	4.34	1.92	2.27	0.439	0.967	4.18	0.196	-
2.50	0.043	13.99	4.29	10.53	11.05	2.34	2.78	0.441	0.965	5.31	0.237	-
2.70	0.048	14.40	4.40	10.43	11.80	2.41	2.86	0.427	0.963	5.70	0.259	0.468
3.00	0.047	15.08	4.76	10.24	14.22	2.55	2.99	0.419	0.934	6.14	0.271	0.446
3.20	0.048	15.59	4.88	10.19	14.95	2.69	3.12	0.408	0.954	6.65	0.257	0.475

Table 5.Heat transfer coefficients resulting from modified Wilson plot method and Cooper correlation at condensing temperature = 30°C for R1234yf

Brine Heat load (kW)	U ((W/K.m²)	T_{LMTD} (evap) (K)	q (W/m²)	$1/(q^{1.1})$	h_r (Wilson plot method) (W/K.m²)	h_r (Cooper correlation) (W/K.m²)
1.00	344.26	8.58	2953.32	0.000152286	415.84	691.82
1.50	464.12	9.52	4420.63	9.77E-05	604.38	1006.26
1.70	527.70	9.27	4893.61	8.74E-05	716.84	1110.77
2.00	593.46	9.61	5700.37	7.39E-05	843.85	1278.37
2.15	587.31	10.26	6028.16	6.95E-05	831.48	1352.23
2.00	550.86	9.90	5452.77	7.76E-05	760.26	1227.95
2.50	738.42	9.69	7156.69	5.75E-05	1170.62	1598.98
2.70	717.90	10.56	7580.47	5.40E-05	1119.87	1687.59
3.00	811.08	9.95	8074.32	5.04E-05	1364.41	1805.22
3.20	838.15	10.13	8493.75	4.76E-05	1442.78	1902.61

Table 6. Heat transfer coefficients resulting from modified Wilson plot method and Cooper correlation at condensing temperature = 40°C for R1234yf

Brine Heat load (kW)	U (W/K.m²)	T_{LMTD} (evap) (K)	q (W/m²)	$1/(q^{1.1})$	h_r (Wilson plot method) (W/K.m²)	h_r (Cooper correlation) (W/K.m²)
1.00	281.81	10.50	2958.10	0.000152015	287.48	703.91
1.50	423.59	10.28	4355.95	9.93E-05	436.54	1017.40
1.70	475.86	10.03	4774.74	8.98E-05	492.26	1126.77
2.00	527.83	10.38	5481.27	7.71E-05	548.08	1269.93
2.15	612.15	9.88	6045.33	6.93E-05	639.56	1414.50
2.00	550.23	10.02	5511.18	7.67E-05	572.27	1280.59
2.50	676.66	10.30	6972.12	5.92E-05	710.30	1632.73
2.70	764.44	9.74	7447.05	5.51E-05	807.66	1749.93
3.00	836.86	9.68	8104.24	5.02E-05	888.94	1925.98
3.20	863.91	9.84	8502.29	4.76E-05	919.51	2000.97

Table 7.Heat transfer coefficients resulting from modified Wilson plot method and Cooper correlation at condensing temperature = 30°C for R134a

Brine Heat load (kW)	U ((W/K.m²)	T_{LMTD} (evap) (K)	q (W/m²)	$1/(q^{1.1})$	h_r (Wilson plot method) (W/K.m²)	h_r (Cooper correlation) (W/K.m²)
1.00	404.01	7.37	2977.48	0.000150927	459.73	688.26
1.50	508.36	8.69	4418.38	9.78E-05	681.62	973.69
1.70	563.52	8.52	4802.64	8.92E-05	784.58	1062.31
2.00	592.91	9.06	5371.49	7.89E-05	842.75	1178.53
2.15	604.71	9.81	5932.50	7.07E-05	866.79	1292.16
2.00	606.37	9.13	5534.01	7.63E-05	870.20	1207.69
2.50	746.66	9.49	7085.20	5.82E-05	1191.48	1533.25
2.70	731.53	10.26	7504.56	5.46E-05	1153.41	1624.50
3.00	802.90	10.07	8084.87	5.03E-05	1341.41	1735.56
3.20	834.61	10.30	8595.69	4.70E-05	1432.32	1853.13

Table 8. Heat transfer coefficients resulting from modified Wilson plot method and Cooper correlation at condensing temperature = 40°C for R134a

Brine Heat load (kW)	U (W/K.m²)	T_{LMTD} (evap) (K)	q (W/m²)	$1/(q^{1.1})$	h_r (Wilson plot method) (W/K.m²)	h_r (Cooper correlation) (W/K.m²)
1.00	482.52	7.26	3501.91	0.00012626	534.06	785.59
1.50	475.22	9.33	4436.14	9.73E-05	525.13	998.50
1.70	562.20	9.37	5268.77	8.06E-05	633.42	1168.01
2.00	765.45	8.65	6623.37	6.26E-05	903.81	1421.42
2.15	808.96	8.93	7226.96	5.69E-05	965.11	1577.63
2.00	659.11	9.38	6183.02	6.76E-05	759.19	1348.64
2.50	765.90	9.85	7544.69	5.43E-05	904.45	1670.38
2.70	828.99	9.39	7782.41	5.25E-05	993.76	1720.90
3.00	867.03	9.50	8237.50	4.93E-05	1048.92	1841.05
3.20	823.11	10.56	8688.06	4.65E-05	985.31	1924.92

Table 9. Heat transfer coefficients of the secondary refrigerant (brine) resulting from Talik et al. correlation and subsequently heat transfer coefficients of R1234yf resulting from equation 46 at condensing temperature = 30°C for R1234yf

Brine Heat load (kW)	U (W/K.m²)	T_{LMTD} (evap) (K)	Re_{brine}	h_{brine} (W/K.m²)	h_r (W/K.m²)
1.00	344.26	8.58	43.1	1397.8	456.75
1.50	464.12	9.52	89.3	2084.8	597.04
1.70	527.70	9.27	97.6	2163.6	697.92
2.00	593.46	9.61	112.2	2260.0	804.78
2.15	587.31	10.26	115.9	2271.0	792.19
2.00	550.86	9.90	104.9	2240.4	730.47
2.50	738.42	9.69	127.3	2177.4	1117.33
2.70	717.90	10.56	130.1	2315.3	1040.54
3.00	811.08	9.95	131.5	2361.0	1235.53
3.20	838.15	10.13	134.5	2383.6	1292.70

Table 10. Heat transfer coefficients of the secondary refrigerant (brine) resulting from Talik et al. correlation and subsequently heat transfer coefficients of R1234yf resulting from equation 46 at condensing temperature = 40°C for R1234yf.

Brine Heat load (kW)	U (W/K.m²)	T_{LMTD} (evap) (K)	Re brine	h brine (W/K.m²)	h_r (W/K.m²)
1.00	281.81	10.50	50.8	1502.1	346.88
1.50	423.59	10.28	74.2	1731.9	560.74
1.70	475.86	10.03	82.9	1800.2	646.84
2.00	527.83	10.38	90.9	1892.5	731.99
2.15	612.15	9.88	95.9	1908.4	901.25
2.00	550.23	10.02	91.4	1901.0	774.35
2.50	676.66	10.30	106.3	1988.1	1025.78
2.70	764.44	9.74	109.1	2038.8	1223.01
3.00	836.86	9.68	117.5	2105.7	1388.84
3.20	863.91	9.84	113.3	2033.7	1501.93

Table 11. Heat transfer coefficients of the secondary refrigerant (brine) resulting from Talik et al. correlation and subsequently heat transfer coefficients of R134a resulting from equation 46 at condensing temperature = 30°C

Brine Heat load (kW)	U ((W/K.m²)	T_{LMTD} (evap) (K)	Re $_{brine}$	h $_{brine}$ (W/K.m²)	h_r (W/K.m²)
1.00	404.01	7.37	40.0	1300.0	586.16
1.50	508.36	8.69	59.8	1601.8	744.71
1.70	563.52	8.52	64.3	1580.7	875.71
2.00	592.91	9.06	71.0	1334.8	1066.74
2.15	604.71	9.81	81.2	1738.5	927.23
2.00	606.37	9.13	72.7	1358.7	1095.08
2.50	746.66	9.49	87.0	1753.1	1300.60
2.70	731.53	10.26	92.6	1834.6	1216.65
3.00	802.90	10.07	93.4	1841.8	1423.40
3.20	834.61	10.30	98.1	1882.2	1499.52

Table 12.Heat transfer coefficients of the secondary refrigerant (brine) resulting from Talik et al. correlation and subsequently heat transfer coefficients of R134a resulting from equation 46 at condensing temperature = 40°C

Brine Heat load (kW)	U (W/K.m²)	T_{LMTD} (evap) (K)	Re brine	h brine (W/K.m²)	h_r (W/K.m²)
1.00	482.52	7.26	55.8	1610.8	689.88
1.50	475.22	9.33	66.1	1614.1	673.51
1.70	562.20	9.37	79.8	1824.9	812.51
2.00	765.45	8.65	103.2	2082.6	1210.29
2.15	808.96	8.93	111.2	2108.7	1312.45
2.00	659.11	9.38	90.5	1887.6	1012.76
2.50	765.90	9.85	104.3	1984.7	1247.20
2.70	828.99	9.39	100.0	1923.1	1457.12
3.00	867.03	9.50	104.7	1962.2	1553.48
3.20	823.11	10.56	102.0	1896.3	1454.43

Appendix B

Table 13.Thermodynamic properties of R1234yf (Lemmon et al., 2010)

		Liquid	Vapor	Liquid	Vapor	Liquid	Vapor	Liquid	Vapor	Liquid	Vapor	Liquid	Vapor	Liquid	Vapor
Temperature	Pressure	Density	Density	Enthalpy	Enthalpy	Entropy	Entropy	Cv	Cv	Cp	Cp	Therm. Cond.	Therm. Cond.	Viscosity	Viscosity
(°C)	(MPa)	(kg/m³)	(kg/m³)	(kJ/kg)	(kJ/kg)	(kJ/kg.K)	(kJ/kg.K)	(kJ/kg.K)	(kJ/kg.K)	(kJ/kg.K)	(kJ/kg.K)	(W/m.K)	(W/m.K)	(Poise)	(Poise)
-50	0.0376	1319	2.363	-24.266	165.83	-0.1038	0.7481	0.7800	0.6875	1.1616	0.7690	0.0942	0.0095	0.0041996	0.00009145
-45	0.0488	1305.8	3.016	-18.421	169.33	-0.0779	0.7450	0.7903	0.7004	1.1746	0.7839	0.0923	0.0099	0.003872	0.000093454
-40	0.0626	1292.3	3.805	-12.510	172.84	-0.0524	0.7426	0.8007	0.7134	1.1879	0.7991	0.0904	0.0103	0.0035824	0.00009545
-35	0.0793	1278.7	4.748	-6.530	176.36	-0.0270	0.7409	0.8113	0.7265	1.2015	0.8149	0.0885	0.0106	0.0033247	0.00009744
-30	0.0993	1264.9	5.866	-0.480	179.87	-0.0020	0.7398	0.8219	0.7398	1.2156	0.8311	0.0867	0.0110	0.0030939	0.000099426
-25	0.1231	1250.8	7.182	5.643	183.38	0.0229	0.7391	0.8325	0.7531	1.2300	0.8478	0.0849	0.0114	0.0028861	0.00010141
-20	0.1512	1236.5	8.719	11.839	186.87	0.0475	0.7389	0.8432	0.7665	1.2449	0.8652	0.0831	0.0118	0.0026979	0.000103 4
-15	0.1840	1221.9	10.504	18.112	190.35	0.0719	0.7392	0.8538	0.7800	1.2602	0.8832	0.0813	0.0122	0.0025265	0.000105 4
-10	0.2221	1207	12.565	24.463	193.81	0.0962	0.7397	0.8644	0.7937	1.2761	0.9020	0.0796	0.0126	0.0023699	0.00010741
-5	0.2659	1191.8	14.934	30.896	197.24	0.1203	0.7406	0.8750	0.8074	1.2925	0.9215	0.0778	0.0131	0.0022259	0.00010945
0	0.3161	1176.3	17.646	37.413	200.64	0.1442	0.7418	0.8854	0.8213	1.3097	0.9421	0.0761	0.0135	0.0020931	0.00011152

5	0.3732	1160.3	20.739	44.018	203.99	0.1680	0.7431	0.8958	0.8351	1.3277	0.9636	0.0745	0.0140	0.00197	0.00011363
10	0.4377	1143.9	24.256	50.713	207.3	0.1916	0.7447	0.9061	0.8491	1.3466	0.9865	0.0728	0.0144	0.0018555	0.00011581
15	0.5104	1127.1	28.248	57.504	210.55	0.2152	0.7463	0.9162	0.8631	1.3666	1.0109	0.0711	0.0149	0.0017485	0.00011807
20	0.5918	1109.7	32.770	64.395	213.73	0.2386	0.7481	0.9263	0.8773	1.3880	1.0373	0.0695	0.0154	0.0016482	0.00012043
25	0.6827	1091.7	37.888	71.392	216.83	0.2620	0.7498	0.9362	0.8918	1.4110	1.0664	0.0679	0.0160	0.0015539	0.00012291
30	0.7835	1073.1	43.680	78.500	219.83	0.2854	0.7516	0.9461	0.9068	1.4360	1.0989	0.0662	0.0165	0.0014647	0.00012556
35	0.8952	1053.7	50.236	85.730	222.73	0.3087	0.7533	0.9560	0.9224	1.4636	1.1357	0.0646	0.0171	0.00138	0.00012852
40	1.0183	1033.5	57.669	93.090	225.49	0.3320	0.7548	0.9658	0.9388	1.4944	1.1780	0.0630	0.0177	0.0012994	0.0001315
45	1.1537	1012.2	66.114	100.590	228.11	0.3553	0.7562	0.9758	0.9560	1.5296	1.2275	0.0614	0.0184	0.0012222	0.00013477
50	1.3021	989.82	75.745	108.260	230.55	0.3788	0.7572	0.9860	0.9742	1.5704	1.2862	0.0597	0.0192	0.001148	0.00013844
55	1.4644	966	86.785	116.100	232.79	0.4024	0.7579	0.9966	0.9933	1.6192	1.3576	0.0581	0.0201	0.0010762	0.0001426
60	1.6415	940.49	99.533	124.160	234.76	0.4262	0.7582	1.0078	1.0134	1.6792	1.4468	0.0565	0.0211	0.0010064	0.00014742
65	1.8343	912.84	114.410	132.460	236.42	0.4503	0.7577	1.0198	1.0348	1.7562	1.5630	0.0548	0.0222	0.00093775	0.00015309
70	2.0440	882.43	132.010	141.070	237.67	0.4749	0.7564	1.0331	1.0578	1.8602	1.7227	0.0531	0.0236	0.00086963	0.00015994
75	2.2717	848.3	153.320	150.080	238.37	0.5002	0.7538	1.0486	1.0832	2.0112	1.9597	0.0515	0.0254	0.00080093	0.00016848

80	2.5191	808.77	179.970	159.650	238.26	0.5266	0.7492	1.0679	1.1125	2.2560	2.3543	0.0499	0.0278	0.00072997	0.00017962
85	2.7877	760.45	215.340	170.090	236.88	0.5550	0.7415	1.0947	1.1491	2.7378	3.1552	0.0486	0.0313	0.00065359	0.00019531
90	3.0804	694.05	268.770	182.270	232.92	0.5876	0.7271	1.1405	1.2030	4.2215	5.6810	0.0484	0.0376	0.0005635	0.00022119

Appendix C

Table 14.Thermodynamic properties of R1234ze (Lemmon et al., 2010)

		Liquid	Vapor	Liquid	Vapor	Liquid	Vapor	Liquid	Vapor	Liquid	Vapor
Temperature	Pressure	Density	Density	Enthalpy	Enthalpy	Entropy	Entropy	Cv	Cv	Cp	Cp
(°C)	(MPa)	(kg/m³)	(kg/m³)	(kJ/kg)	(kJ/kg)	(kJ/kg-K)	(kJ/kg-K)	(kJ/kg-K)	(kJ/kg-K)	(kJ/kg-K)	(kJ/kg-K)
-50	0.0210	1374.5	1.307	-38.34	173.36	-0.161	0.788	0.807	0.672	1.201	0.750
-45	0.0280	1362.0	1.711	-32.30	176.87	-0.134	0.783	0.815	0.683	1.211	0.763
-40	0.0368	1349.3	2.210	-26.22	180.39	-0.107	0.779	0.822	0.695	1.222	0.777
-35	0.0477	1336.4	2.818	-20.08	183.92	-0.081	0.775	0.830	0.707	1.233	0.791
-30	0.0611	1323.3	3.553	-13.88	187.45	-0.056	0.772	0.838	0.719	1.244	0.805
-25	0.0773	1310.1	4.433	-7.63	190.98	-0.030	0.770	0.846	0.732	1.255	0.820
-20	0.0968	1296.6	5.476	-1.31	194.51	-0.005	0.768	0.855	0.744	1.267	0.836
-15	0.1200	1282.9	6.704	5.06	198.03	0.020	0.767	0.863	0.757	1.280	0.852
-10	0.1474	1269.0	8.140	11.50	201.53	0.044	0.766	0.872	0.770	1.292	0.868
-5	0.1793	1254.8	9.807	18.00	205.02	0.069	0.766	0.880	0.783	1.306	0.886
0	0.2165	1240.3	11.733	24.58	208.49	0.093	0.766	0.889	0.797	1.320	0.904
5	0.2593	1225.5	13.946	31.23	211.93	0.117	0.767	0.898	0.810	1.335	0.923
10	0.3083	1210.4	16.480	37.95	215.34	0.141	0.767	0.907	0.824	1.350	0.943
15	0.3641	1194.9	19.368	44.75	218.70	0.164	0.768	0.916	0.838	1.366	0.964
20	0.4273	1179.0	22.650	51.64	222.03	0.188	0.769	0.926	0.852	1.384	0.986
25	0.4986	1162.7	26.371	58.61	225.30	0.211	0.770	0.935	0.866	1.402	1.009
30	0.5784	1145.9	30.581	65.68	228.51	0.235	0.772	0.944	0.880	1.422	1.034
35	0.6676	1128.5	35.338	72.84	231.65	0.258	0.773	0.954	0.894	1.443	1.061
40	0.7666	1110.6	40.709	80.11	234.70	0.281	0.774	0.963	0.908	1.466	1.090

45	0.8764	1092.0	46.775	87.50	237.65	0.304	0.776	0.973	0.922	1.492	1.123
50	0.9975	1072.7	53.629	95.00	240.48	0.327	0.777	0.982	0.937	1.520	1.160
55	1.1308	1052.5	61.388	102.64	243.16	0.350	0.778	0.992	0.954	1.553	1.205
60	1.2769	1031.2	70.191	110.43	245.69	0.373	0.779	1.002	0.972	1.589	1.258
65	1.4368	1008.8	80.216	118.39	248.03	0.396	0.780	1.013	0.992	1.632	1.323
70	1.6113	984.9	91.694	126.53	250.15	0.420	0.780	1.025	1.015	1.684	1.403
75	1.8014	959.3	104.930	134.90	252.00	0.443	0.780	1.037	1.039	1.748	1.503
80	2.0080	931.5	120.360	143.53	253.53	0.467	0.779	1.052	1.065	1.831	1.633
85	2.2323	900.9	138.620	152.49	254.62	0.492	0.777	1.068	1.092	1.944	1.811
90	2.4757	866.4	160.720	161.88	255.13	0.517	0.774	1.087	1.122	2.108	2.075
95	2.7396	826.3	188.420	171.88	254.79	0.544	0.769	1.110	1.156	2.378	2.519
100	3.0261	776.8	225.360	182.84	253.04	0.572	0.760	1.143	1.199	2.922	3.438

Appendix D

Table 15 .Thermodynamic properties of Ethylene glycol 25.3 wt% with freezing point temperature of -12ºC (Melinder Å., 2010)

Temperature (ºC)	Cp (J/kgK)	Density ϱ (kg/m³)	Viscosity μ (mPa.s)	Pr	Thermal conductivity (W/m.K)
40	3852.2	1024.8	1.187	9.226	0.496
20	3799.6	1033.3	1.963	15.604	0.477
10	3770.2	1036.6	2.684	21.670	0.467
0	3740.9	1039.3	3.843	31.483	0.457
-10	3714.8	1041.3	5.897	49.091	0.446

Appendix E

Refrigerants Safety Group Classifications (ASHRAE Standard, 2010):

The safety classification contains two alphanumerical characters (like A2); the capital letter shows toxicity and the number indicates flammability level.

Toxicity classification:

Class A: toxicity has not been identified at concentrations ≤ 400 ppm, based on TLV.

Class B: there is evidence of toxicity at concentrations below 400 ppm, based on TLV.

Flammability Classification:

Class 1: No flame propagation in air at 21°C and 1.01 bar

Class 2: Lower flammability level, LFL > 0.10 kg/m³ at 21°C and 1.01 bar and heat of combustion < 19 000 kJ/kg

Class 3: Highly flammable, LFL ≤ 0.10 kg/m³ at 21°C and 1.01 bar and heat of combustion ≥ 19 000 kJ/kg

Optional subclass 2L:

Those low flammable refrigerants which meet following additional condition:

A maximum burning velocity of ≤10 cm/s at 23 °C and 1.01 bar

Flammability	Toxicity	
	Lower	Higher
No Flame propagation	A1	B1
Lower flammability	A2	B2
	A2L	B2L
Higher flammability	A3	B3